Available online at www.sciencedirect.com
SCIENCE DIRECT
ELSEVIER
Coordination Chemistry Reviews 249 (2005) 2232–2258
COORDINATION CHEMISTRY REVIEWS
www.elsevier.com/locate/ccr

Review

Copper(I), silver(I) and gold(I) carboxylate complexes as precursors in chemical vapour deposition of thin metallic films

A. Grodzicki, I. Łakomska, P. Piszczek, I. Szymańska, E. Szłyk *

Nicolaus Copernicus University, Faculty of Chemistry, Gagarina 7, 87-100 Toruń, Poland

Received 29 October 2004; accepted 29 May 2005
Available online 19 July 2005

Contents

Abstract

Volatile precursors of copper, silver and gold for chemical vapour deposition (CVD) of metallic layers are described. There is considerable research interest in CVD because it provides advantages such as selective deposition, control of film density and thickness, etc. over other physical deposition techniques. Copper, silver, and gold compounds used as CVD precursors can be divided into three types: inorganic, coordination and organometallic. Organometallic compounds are often used as CVD precursors, however they usually are air and moisture sensitive, moreover they are characterized by low thermal stability. Inorganic compounds, which are usually air stable and easy to obtain, exhibit low volatility and require lower deposition pressures and higher vapourization temperatures. Therefore, we present here results on: (a) synthesis and characterization of inorganic and coordination precursors, (b) applications in CVD of metallic layers, (c) studies on the impact of CVD parameters on the quality of nanolayers, (d) gas phase composition and reactions during fabrication of the metallic films.

Carboxylates of copper(I), silver(I) and gold(I) and their complexes with tertiary phosphines are described as a new class of CVD precursor. The molecular structures have been discussed based on X-ray structural analysis and spectroscopic methods. ^{1}H, ^{13}C, ^{31}P, ^{19}F, ^{63}Cu NMR ^{31}P CP MAS NMR, along with variable temperature NMR and IR were used for characterization of new Cu(I), Ag(I) and Au(I) complexes of general formula [M (COOR)(L)] where R = CH_3, $C(CH_3)_3$, C_2F_5, C_2H_5, $(CH_3)_3SiCH_2$, C_3H_7, C_3F_7, $(CH_3)_3SiC_2H_4$, C_4H_9, C_6F_{13}, C_7F_{15}, C_8F_{17}, C_9F_{19}, C_6F_5, $C_6H_2(CH_3)_3$, L = PR′ where R′ = Me, Et, Ph, OMe, OEt, OPh, or L = diphosphines—dppm, dppe. The analyses of thermal

* Corresponding author. Tel.: +48 56611 43 16; fax: +48 56654 24 77.
E-mail address: eszlyk@chem.uni.torun.pl (E. Szłyk).

doi:10.1016/j.ccr.2005.05.026

decomposition and MS data have been used for elucidation of the decomposition mechanisms, description of the transport in the gas phase and deposition processes. The molecular structures of the precursors have been discussed in relation to the quality of the obtained metallic nanolayers.

Keywords: Copper(I); Silver(I); Gold(I); Volatile carboxylate complexes; Phosphines; CVD

1. Introduction

The synthesis and characterization of copper, silver and gold coordination compounds as new precursors for chemical vapour deposition (CVD) of metallic thin layers is an area of extensive research. The fabrication of metallic thin films using CVD techniques is a matter of interest, due to advantages arising, among others, from kinetically controlled deposition processes. The unique structural, optical and electrical properties of these metals have resulted in their wide applications including the vertical interconnects in microelectronic devices [1–3], ultrafast optical switches [4], optical filters [5,6] and components of high-temperature superconducting materials [7]. Metallic films can be produced by many deposition techniques, e.g. galvanic, sol–gel [8], photochemical deposition [9], thermal evaporation [10], or pulsed laser deposition [11]. The development of these methods requires stable volatile metallic compounds, which can act as precursors of the metals. Copper, silver and gold compounds used as CVD precursors are classified into three types: inorganic [12,13], organometallic [1,13,14] and coordination [13,15,16].

In addition to the physical deposition parameters, the properties of nanofilms can also be controlled by the molecular nature of the process. The CVD of an elemental material such as a metal is simple, but it can be complicated when another molecular precursor is introduced and binary and ternary materials can be obtained (alloys). Selected precursors can produce a uniform coating on a complex surface of substrate. This can be achieved by phase diffusion of precursors and penetration of the complex substrate surface. These characteristic features prompted us to prepare and structurally characterize coordination precursors of copper, silver and gold.

Organometallic compounds are often used as CVD precursors, however they usually are air and moisture sensitive, moreover they exhibit low thermal stability. On the other hand they demonstrate better volatility (deposition temperature <300 °C), in comparison to inorganic precursors; however non-metallic impurities in films (e.g. C, O, F, P, N) can be a significant problem in microelectronic technologies. However, the use of hydrogen as a reduction component of the carrier gas, contributes to a significant decrease in the non-metallic impurities in metallic layers. The majority of inorganic compounds, because they are involatile and require low deposition pressures (below 10^{-2} mbar) at higher vapourization temperatures (above 400 °C), can be obtained in a simpler way and are air stable.

Therefore in this review the following areas of research will be discussed: (a) synthesis and characterization of the inorganic and coordination precursors, (b) applications of these precursors in CVD of metallic layers, (c) the impact of CVD parameters on the quality of nanolayers, (d) gas phase composition and reactions during fabrication of the metallic films. The parameters that decide the use of a particular compound as a precursor are as follows: sufficient thermal stability, volatility that enables transport to a substrate and high purity of metallic layers.

The most general feature, which has an impact on the volatility of compounds, is their molecular structure. Therefore the potential precursors should be: non ionic, with weak intermolecular interactions and decompose to pure metallic films under strictly defined temperature and pressure conditions. In the design of precursors for pyrolitic CVD applications, knowledge about the gas phase reactions enables fabrication of pure metallic surfaces. Ligand dissociation and fragmentation reactions in the gas phase have the principal impact on the purity of films. Therefore, the additional goal was to describe the mechanisms of decomposition in the solid state and elucidation of the gas phase molecular composition during transport in the CVD process.

The most often used inorganic precursors of copper, silver and gold are fluorinated Au(I), Ag(I) and Cu(I) β-diketonates, and their complexes with secondary ligands which stabilize M–O bonds. Soft donors e.g. P-, S- and olefins are used most often as secondary ligands. The systematic variation of ligands, by changing the β-diketonate and the secondary ligand can result in obtaining the required film properties. A number of complexes with empirical formula M(β-diketonate)L, where M = Cu, Ag, Au; L=PR'_3, R′ = Me, Et or alkynes, vinyltrimethylsilane (VTMS); (β-diketonate) = 2,2-dimethyl-6,6,7,7,8,8,8-heptafluoro-3,5-octanedionato (fod), 1,1,1,5,5,5-hexfluoroacetylacetonato (hfac) or silanes were applied [1,2,14–23]. The best volatility and stability of complexes were noted for fluorinated β-diketonates and low molecular weight tertiary phosphines. Fluorinated Schiff base analogous of β-diketonates have also been employed as precursors, but they were less volatile than the β-diketonates [18].

In order to find suitable inorganic precursors, research interest has focused on noble metal carboxylates and their complexes. The primary ligands in these complexes were σ-bonded aliphatic and perfluorinated aliphatic carboxylates. The secondary ligands usually were tertiary phosphines, which belong to end-on σ-donor, π-acceptor ligands, which are particularly useful in stabilizing the coordination sphere

of soft metals such as Cu(I), Ag(I), Au(I) [24–27]. Such ligand systems should decompose easily on the σ-donor end, while being stabilized on the π-acceptor side during decomposition and transport processes. Moreover, Ag(I) ions demonstrate a variable nuclearity in the phosphine complexes which make them an attractive subject for structural studies. Perfluorinated aliphatic carboxylates have been chosen as O-donor ligands because fluorine improve the volatility of complexes, which is important for CVD experiments. Moreover, carboxylates are able to bind in mono- or polydentate (chelating or bridging) mode; hence one may expect multinuclear complexes [28]. In the case of perfluorinated carboxylates, due to lower basicity of COO group than for the non-fluorinated analogs, different coordination modes can also be expected. Additionally the diamagnetism of Cu(I), Ag(I) and Au(I) complexes, allows characterization in the solid state with ^{1}H, ^{13}C CP MAS NMR and in solution by ^{1}H, ^{13}C, ^{19}F, ^{31}P, ^{63}Cu NMR, along with variable temperature NMR. The detailed analysis of the ^{1}H, ^{13}C, ^{19}F, ^{31}P NMR resonance and the spin–spin coupling have been used for elucidation of the geometry of the complexes and ligand coordination modes in solution, whereas IR and ^{31}P CP MAS NMR spectroscopy were used for the same purpose in the solid state [29–46].

2. Copper(I) carboxylate complexes

Copper(I) complexes with oxygen donor ligands such as carboxylates exhibit mono- or multinuclear structures depending on the nature of the carboxylate and other ligands in the coordination sphere. These compounds have been studied less than analogous Cu(II) species, due to the instability of copper(I)–oxygen bonds. One can explain this as a weak bond between hard oxygen and soft Cu(I) using hard–soft acid–base theory. The copper(I) carboxylates exhibited tetrameric (e.g. $[CuOOCCF_3]_4{\cdot}2C_6H_6$) or polymeric (e.g. $[CuOOCCH_3]_n$) structures in the solid state [47–54] and are air and moisture sensitive. The complexes increased in stability when olefins, amines, phosphites or phosphines were introduced to the coordination sphere.

2.1. Copper(I) carboxylate complexes with tertiary phosphines

Copper(I) carboxylate complexes have many applications: in catalytic processes [55–66], in host–guest chemistry [67] and in medicine [68]. Dicopper(I) oxalate complexes with alkynes or alkenes [69] have been studied as precursors in CVD of thin copper films.

Copper(I) carboxylate complexes with phosphines were obtained as follows: the reduction of copper(II) carboxylates by various reducing agents (e.g. phosphines, metallic copper, hydrazine) [29–34,61,63,70], electrochemical oxidation of copper metal in the presence of phosphine and carboxylic acid [71], the reaction of carbon dioxide with alkyl- or aryl-

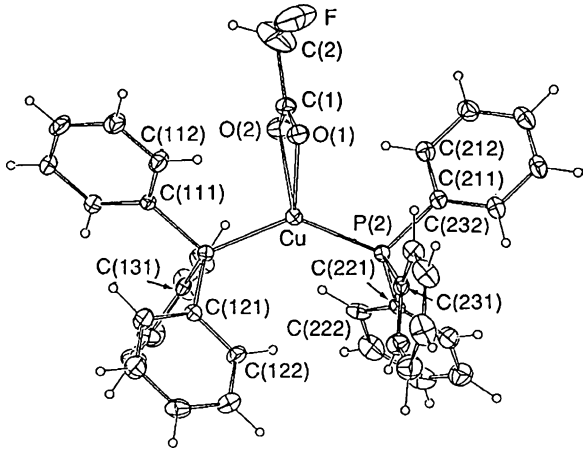

Fig. 1. Structure of $[Cu(OOCCFH_2)(PPh_3)_2]$ (reprinted with permission from Ref. [71]; Copyright 1994 RSC).

copper(I) compounds [60,62,64,66] and the exchange with carboxylates in copper(I) salts [59,61,65]. Cu(I) carboxylates complexes with triphenylphosphine were most intensively studied. The monomeric $[Cu(OOCR)(PPh_3)_2]$, where R = H, CH_3, $C_6H_5CONHCH_2$, $CH_2{=}CHCH_2$, fluorene and CFH_2, exhibited a distorted tetrahedral geometry of Cu(I), with varying degrees of asymmetry and bidentately linked carboxylates [60,61,70–74]. An X-ray structure is shown in Fig. 1, illustrating the chelating monofluoroacetate in a complex with triphenylphosphine.

Analogous structures were proposed for $[Cu(OOCR)(PPh_3)_2]$, R = Et, *n*-Pr, *i*-Bu, Ph, *o*-tol, *m*-tol, *p*-tol from spectroscopic and conductivity data [60,62]. In the case of di- and trifluoroacetate $[Cu(OOCR)(EtOH)(PPh_3)_2]$, Cu–O bonds were asymmetric, such that the carboxylate appeared to be monodentately coordinated and ethanol molecule has completed the coordination sphere (Fig. 2) [63,71]. Similarly, a monodentate carboxylate binding mode was observed for

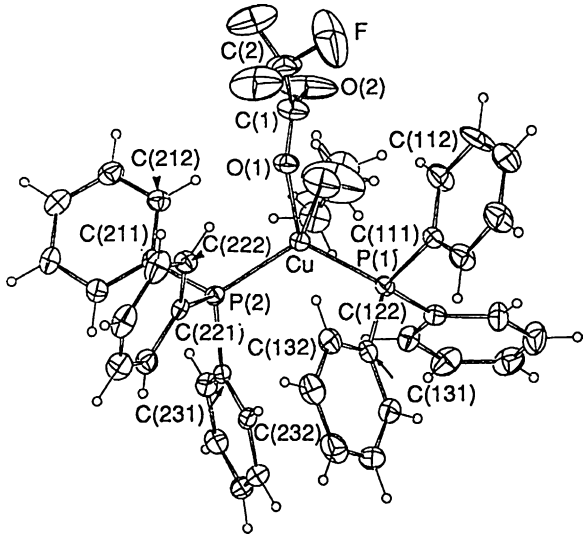

Fig. 2. Structure of $[Cu(OOCCF_3)(EtOH)(PPh_3)_2]$ (reprinted with permission from Ref. [71]; Copyright 1994 RSC).

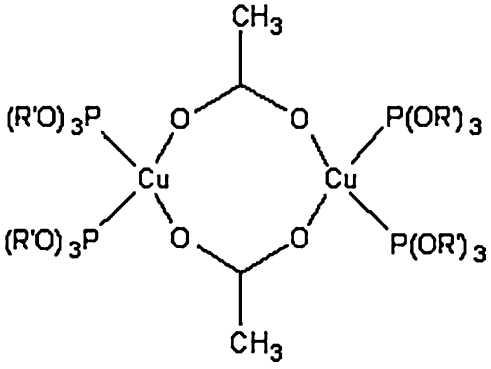

Fig. 3. Structure of $[Cu_2\{P(OR')_3\}_4(\mu\text{-}OOCCH_3)_2]$ (reprinted with permission from Ref. [57]; Copyright 1981 RSC).

other carboxylates: orotates, dihydroorotates and cyanoacetate, where tricoordinated Cu(I) ions were observed [64,65].

The complexes $[Cu(OOCH)(PPh_3)_3]\cdot HCOOH$ and $[Cu(OOCH)(PPh_3)_3]\cdot 0.5EtOH$ exhibit four-coordinated Cu(I) with three crystallographically independent phosphine molecules and monodentate formate anion. The ^{31}P CPMAS NMR spectra of these complexes exhibit partially resolved multiplets resulting from an inequivalence of the triphenylphosphines [75]. The analogous structure was evident for [Cu(OOCH)(triphos)]. Moreover the spectroscopic data suggested different types of formate bonding (monodentate, chelate or bridging) depending on the type of phosphine (PPh_3, PCy_3, $PMePh_2$, etp_3) and synthesis conditions [66].

Liquid compounds of general formulae $[Cu\{P(OR')_3\}_2(\mu\text{-}OOCCH_3)]$, where R′ = Me or Et, were obtained in the reaction of the mixed-valence complexes $[Cu^{I}Cu^{II}_2(OOCCH_3)_5\{P(OR')_3\}_2]$, with monodentate oxygen- or nitrogen-donor ligands, L (e.g. pyridine, urea, triphenylphosphine oxide). The spectroscopic data demonstrate the dimeric structure of the complexes with the bidentate *syn–syn* carboxylates (Fig. 3) [55–57].

Cu(I) complexes with tertiary phosphites and aliphatic perfluorinated carboxylates of the type $[Cu\{P(OR')_3\}(\mu\text{-}OOCR)]$ were prepared as viscous liquids according to the following schemes:

$$[Cu(OOCR)_2] + Cu \rightarrow 2[Cu(OOCR)]_{sol}, \quad (I)$$

$$[Cu(OOCR)]_{sol} + P(OR')_3 \rightarrow [Cu\{P(OR')_3\}(\mu\text{-}OOCR)], \quad (II)$$

where R = CF_3, C_2F_5, C_3F_7, C_6F_{13}, C_7F_{15}, C_8F_{17}, C_9F_{19}: sol = acetonitrile R′ = Ph, Me, Et, *n*-Bu [29,30].

The spectroscopic results suggest a dimeric structure for complexes $[Cu_2\{P(OR')_3\}_2(\mu\text{-}OOCR)_2]$ in the liquid state, where the metal ions in trigonal symmetry are linked by the bridging carboxylates. This type of bonding was also detected in the gas phase by means of VT IR and EIMS spectra analysis. In MS the most intense signals were observed for $[Cu_2(OOCR)]^+$ and $[Cu_2(OOCR)_2]^+$ fragments. The ^{13}C, ^{19}F, ^{31}P and ^{63}Cu NMR spectra were used for elaboration of the exchange processes in acetonitrile solution of $[Cu_2\{P(OPh)_3\}_2(\mu\text{-}OOCR)_2]$ (Fig. 4). Moreover, the copper(I) relaxation processes in these equilibria were sufficiently slow to record a ^{63}Cu NMR signal, which was the first example of symmetry lower than T_d for Cu(I) complexes with $P(OPh)_3$.

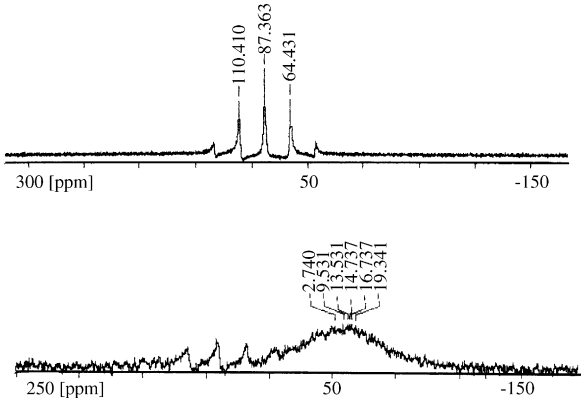

Fig. 4. ^{63}Cu NMR spectra of (a) $[Cu_2\{P(OEt)_3\}_2(\mu\text{-}OOCC_2F_5)_2]$—signal of a cation $[Cu\{P(OEt)_3\}_4]^+$ was detected at 87.4 ppm, (b) $[Cu_2\{P(OBu)_3\}_2(\mu\text{-}OOCC_2F_5)_2]$—signal of a cation $[Cu\{P(OBu)_3\}_4]^+$ and average signal of species $[Cu(OOCC_2F_5)(MeCN)_x]$ ($x = 2$ or 3), $[Cu(MeCN)_2(\mu\text{-}OOCC_2F_5)]$, $[Cu(OOCC_2F_5)(MeCN)_x\{P(OBu)_3\}]$ ($x = 1$ or 2) were detected at 88 and −13 ppm, respectively (reprinted with permission from Ref. [30]; Copyright 1999 Elsevier).

In the case of complexes with alkylphosphite (R′ = Me, Et, Bu) the dimeric structure was broken, into the following species: $[Cu\{P(OR')_3\}_4]^+$, $[Cu(OOCR)(MeCN)_x]$ ($x = 2$ or 3), $[Cu(MeCN)_2(\mu\text{-}OOCR)]$ and $[Cu(OOCR)(MeCN)_x\{P(OR')_3\}]$ ($x = 1$ or 2) (Fig. 5). The signal of a cation $[Cu\{P(OEt)_3\}_4]^+$ (at 87.4 ppm, spectrum a) appeared as a quintet due to the CuP_4 chromophore and heteronuclear spin–spin coupling ($^1J_{Cu-P}$). In the case of $[Cu_2\{P(OBu)_3\}_2(\mu\text{-}OOCC_2F_5)_2]$ (spectrum b) the signal due to the cation $[Cu\{P(OBu)_3\}_4]^+$ was centered at ca. 88 ppm, whereas other species present in solution such as $[Cu(OOCC_2F_5)(MeCN)_x]$ ($x = 2$ or 3), $[Cu(MeCN)_2(\mu\text{-}OOCC_2F_5)]$, $[Cu(OOCC_2F_5)(MeCN)_x\{P(OBu)_3\}]$ form a very wide band centered at ca. −13 ppm.

Thermal studies of two series of compounds: $[Cu(OOCC_2F_5)\{P(OPh)_3\}_m]$ and $[Cu(OOCC_6F_{13})\{P(OPh)_3\}_m]$, $m = 1$–4, exhibited $Cu_2P_2O_7$ as the major product of decomposition, hence they are not suitable for CVD applications [31].

The complexes of general formula $[Cu\{P(OR')_3\}(\mu\text{-}OOCR)]$ were unstable in air, turning green according to the following reaction:

$$4[Cu\{P(OR')_3\}(\mu\text{-}OOCR)] + 2H_2O + O_2 \rightarrow 4[Cu\{P(OR')_3\}(\mu\text{-}OH)(\mu\text{-}OOCR)].$$

EPR spectra and magnetic susceptibility measurements indicate that these complexes have a polymeric structure $[Cu\{P(OR')_3\}(\mu\text{-}OH)(\mu\text{-}OOCR)]_n$ with bridging carboxy-

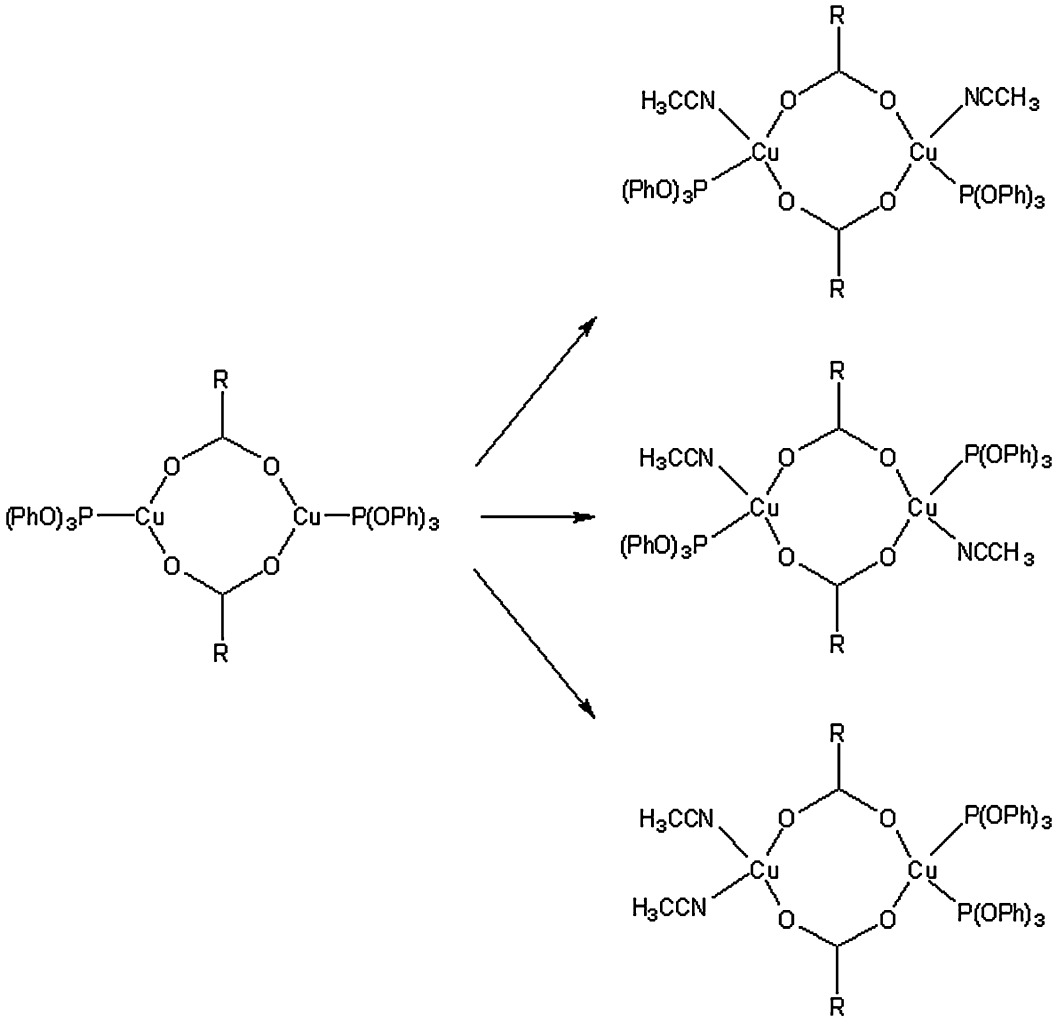

Fig. 5. Possible species existing in equilibrium after dissolving $[Cu(\mu\text{-}OOCR)\{P(OPh)_3\}]_2$ in acetonitrile.

lates and hydroxo group, exhibiting the rarely observed Cu(II)–P(III) bond with monodentately bound phosphite. Thermal decomposition was found to be a multistage process, which in nitrogen yields a mixture of Cu, Cu_2O and $Cu_2P_2O_7$, but in air pure $Cu_2P_2O_7$ [76–78].

X-ray crystal studies of Cu(I) complexes with the ligands discussed are listed in Table 1. The most common structure appears to be monomeric with Cu(I) in a distorted tetrahedral geometry. The distortion is evident in the Cu–P distances, the shortest being 2.219 Å, while the longest 2.341 Å. This suggests uneven bond strength, even with ligands with the same σ-donor, π-acceptor properties (e.g. PPh_3). The same trend can be noted for Cu–O bonds, which are also different, whereas in some cases they are even shorter than Cu–P. This is evident for perfluorinated carboxylates where one Cu–O bond is shorter, but in some cases: $[Cu(OOCCF_3)(EtOH)(PPh_3)_2]$, $[Cu(OOCCF_3)(EtOH)(PPh_3)_2]$ both are shorter than Cu–P. The biggest distortion of P–Cu–P angle is noted for complexes with bulky phosphines (PCy_3). Distortion of the coordination sphere geometry depends strongly on the bulkiness of the phosphines, while variation in metal–ligand bond distances depend on the donor properties of the carboxylates.

2.2. Copper(I) carboxylate complexes with diphosphines

Complexes with diphosphine ligands discussed in this section present more complicated structures than their phosphine analogous. The molecular structure of $[Cu_2(dppm)_2(\mu\text{-}OOCCH_3)]BF_4\cdot(CH_3)_2CO$ exhibits two Cu(I) atoms bridged by two dppm ligands and one acetate, that imposes a tricoordinated metal in a quasi-planar triangular fashion (Fig. 6) [58,79]. The complexes $[Cu_2(OOCR)_2(\mu\text{-dppm})]$, where R = Ph, *o*-tol, *m*-tol, *p*-tol are probably monomers with the bridging diphosphine and bidentate carboxylates, but in the case of complexes $[Cu(OOCR)(\mu\text{-dppm})]$ (R = Ph, *o*-tol, *m*-tol, *p*-tol) dimeric forms with monodentate carboxylates were suggested [60].

For copper(I) perfluorinated carboxylates complexes with dppm $[Cu_2(\mu\text{-dppm})_3(OOCR)_2]$ dppm, where $R = C_2F_5$, C_4F_9, C_6F_{13}, C_8F_{17}, C_9F_{19} a dimeric structure in the solid

Table 1
X-ray crystal structure data for Cu(I) carboxylate complexes with phosphines

Compounds	Type of structure	Bond distances [Å]		Angles [°]			Ref.
		Cu—P	Cu—O	P—Cu—P	P—Cu—O	O—Cu—O	
$[Cu(OOCCH_3)(PPh_3)_2]$ ($T = 193$ K)	Monomeric (distorted tetrahedral)	2.224(1); 2.231(1)	2.228(3); 2.166(3)	133.3(1)	[a]	60.3(1)	[61]
$[Cu(OOCC_6H_5CONHCH_2)(PPh_3)_2]$	Monomeric (distorted tetrahedral)	2.267(5); 2.236(5)	2.136(5); 2.370(6)	130.9(1)	113.9(2); 107.9(2); 113.6(2); 106.6(2)	[a]	[61]
$[Cu(OOCCH_2 = CHCH_2)(PPh_3)_2]$	Monomeric (distorted tetrahedral)	2.241(1); 2.254(1)	2.229(3); 2.194(3)	127.3(1)	108.5(1); 108.7(1); 111.0(1); 119.7(1)	[a]	[61]
$[Cu(OOCC_{13}H_8)(PPh_3)_2]Et_2O$	Monomeric (distorted tetrahedral)	2.238(3); 2.236(3)	2.29(1); 2.156(6)	128.6(1)	110.6(2); 112.9(2); 115.2(2); 112.7(2)	[a]	[61]
$[Cu(OOCC_3H_7)(Pcy_3)_2]$	Monomeric (distorted tetrahedral)	2.231(1); 2.248(1)	2.276(4); 2.181(3)	137.4(1)	102.3(1); 109.4(1); 109.7(1); 111.3(1)	[a]	[65]
$[Cu(OOCC_2H_4CN)(Pcy_3)_2]$	Monomeric (distorted trigonal planar)	2.229(2); 2.243(3)	2.119(7)	145.2(1)	102.8(1); 111.7(2)		[65]
$[Cu(OOCCFH_2)(PPh_3)_2]$	Monomeric (distorted tetrahedral)	2.232(3); 2.222(3)	2.144(6); 2.363(7)	135.0(1)	112.8(2); 101.7(2); 106.8(2); 117.0(2)	58.4(2)	[71]
$[Cu(OOCCF_2H)(PPh_3)_2]$	Monomeric (distorted tetrahedral)	2.234(3); 2.219(2)	2.118(4); 2.465(6)	135.8(1)	111.6(2); 99.3(2); 109.3(2); 117.0(2)	56.7(2)	[71]
$[Cu(OOCCF_3)(PPh_3)_2]$	Monomeric (distorted tetrahedral)	2.235(2); 2.228(2)	2.113(4); 2.545(5)	136.7(1)	112.6(1); 98.6(1); 108.3(1); 116.3(1)	55.4(1)	[71]
$[Cu(OOCCF_2H)(EtOH)(PPh_3)_2]$	Monomeric (distorted tetrahedral)	2.248(3); 2.236(3)	2.074(8); 2.169(8) Cu-EtOH	120.5(1)	107.7(2); 107.7(4); 109.9(2); 116.9(3)	89.4(2)	[71]
$[Cu(OOCCF_3)(EtOH)(PPh_3)_2]$	Monomeric (distorted tetrahedral)	2.248(2); 2.240(2)	2.104(6); 2.160(6) Cu-EtOH	120.8(1)	107.7(2); 107.7(3); 109.1(2); 117.3(2)	89.4(2)	[71]
$[Cu(OOCH)(PPh_3)_2]$	Monomeric (distorted tetrahedral)	2.247(1)	2.226(3)	128.3(4)	[a]	[a]	[60]
$[Cu(OOCH)(PPh_3)_3]\cdot HCOOH$	Monomeric (distorted tetrahedral)	2.315(1); 2.329(1); 2.332(1)	2.085(3)	112.72(4); 115.42(4); 119.45(4)	109.77(9); 98.36(9); 97.35(8)		[75]
$[Cu(OOCH)(PPh_3)_3]\cdot 0.5EtOH$	Monomeric (distorted tetrahedral)	2.332(1); 2.332(1); 2.341(1)	2.042(4)	112.29(4); 116.09(4); 117.98(4)	106.4(2); 101.3(1); 99.8(2)		[75]
$[Cu(OOC_5H_3N_2O_4)(PPh_3)_2]\cdot MeOH$	Polymeric (distorted tetrahedral)	2.255(6); 2.257(8)	2.08(2); 2.28(2) Cu–O exocyclic	[a]	[a]		[64]
$[Cu(OOC_5H_5N_2O_4)(PPh_3)_2]\cdot MeOH$	Monomeric (distorted tetrahedral)	2.260	2.043(4); 2.244(4); 2.200(3); Cu–O exocyclic; 2.245(4) Cu–O exocyclic	[a]	[a]		[64]

[a] Data unavailable.

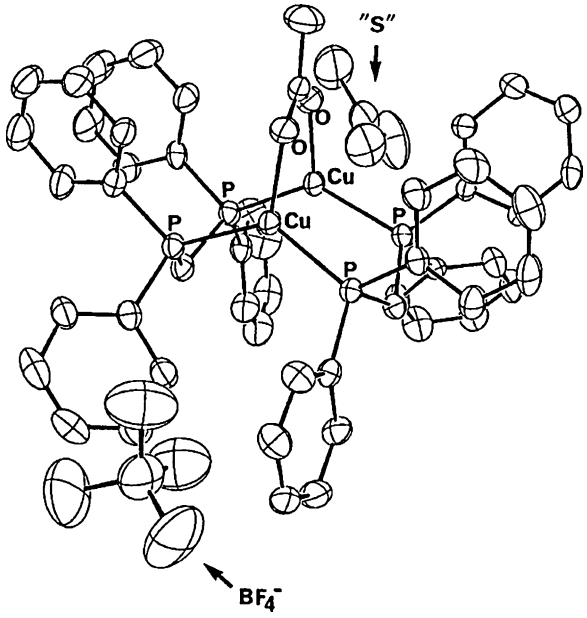

Fig. 6. Structure of $[Cu_2(\mu\text{-}OOCCH_3)(\mu\text{-}dppm)_2]BF_4\cdot(CH_3)_2CO$ (reprinted with permission from Ref. [58]; Copyright 1997 ACS).

state was proposed, with three bridging diphosphines and monodentate carboxylates. This was based upon IR, MS, ^{31}P CPMAS NMR and ^{13}C CPTOSSB NMR analysis. In solution VT ^{31}P NMR spectra exhibited at least three dimeric forms with the most favourable $[Cu(dppm)_2]^+$ species being in equilibrium [32].

Complex $[Cu_2(OOCC_6H_5)_2(dppe)_2(\mu\text{-}dppe)]\cdot 4H_2O$ exhibited two Cu(I) ions bridged by one dppe. The distorted tetrahedral coordination around the Cu(I) is completed by P atoms from the chelating dppe and an O atom from monodentate benzoate (Fig. 7) [68]. Previously, similar structures were proposed for derivatives of $[Cu_2(OOCR)_2(dppe)_2(\mu\text{-}dppe)]$, where R = Me, Ph, *o*-tol, *m*-tol, *p*-tol [60,80]. Moreover, the structure of the complex $[Cu_2(\mu\text{-}OOCCH_3)_2dppe]$ was determined in the solid state, as a polymeric chain of dimeric copper(I) units containing the bridging dppe and two acetates. The dimers were linked via weak Cu–O(carboxylate) interactions [80].

Compounds of general formula $[Cu_2(dppe)_2(\mu\text{-}OOCR)_2]$ and $[Cu(diphosphine)_2](RCOO)$, where $R = C_2F_5$, C_4F_9, C_6F_{13}, C_8F_{17}, C_9F_{19}; diphosphine = dppe, dppp, dppB, were characterized by spectroscopic methods. The presence of distinct bis-chelated cations of $[Cu(diphosphine)_2]^+$, and uncoordinated carboxylate anions has been proposed for M:L = 1:2 complexes in the solid state and in acetonitrile solution. Whereas for M:L = 1:1, a dimeric form with bridging carboxylates and chelating diphosphines in the solid state was postulated. Moreover, in acetonitrile solution VT ^{31}P NMR spectra exhibited at least the following species: $[Cu_2(dppe)_2(\mu\text{-}OOCR)_2]$, $[Cu_2(dppe)_2(OOCR)]^+$, $[Cu(OOCR)(dppe)]$, $[Cu(dppe)_2]^+$ being in equilibrium [33,34].

X-ray crystal data for diphosphines are listed in Table 2. In comparison to monophosphines they exhibit dinuclear and polymeric structures, which are more favourable for bidentate ligands such as diphosphines. The central ions are often in a distorted tetrahedral coordination, while Cu–P distances were in the range 2.157–2.304 Å, whereas Cu–O are shorter, in the range 1.993–2.127 Å. In comparison to monomeric structures with PR_3, the Cu–P bond distances (the shortest being 2.219 Å while the longest 2.341 Å) are slightly longer, whereas for Cu–O the opposite trend is evident. These differences in metal–ligand distances can be connected to the observed stronger thermal stability of diphosphine complexes relative to phosphines. Spectroscopic studies of other diphosphine complexes are also in favour of dimeric or polymeric structures. The low volatility of diphosphine complexes and their lack of CVD applications are a consequence of these more complex structures.

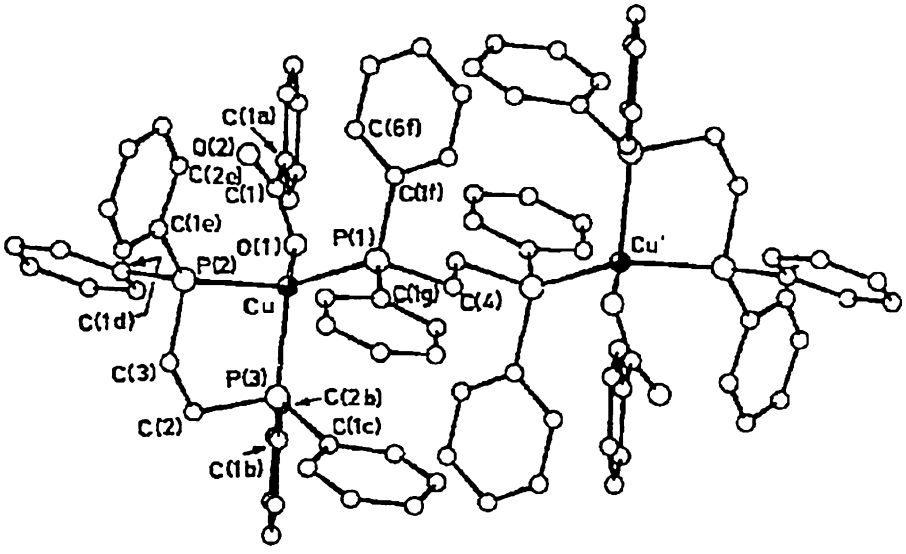

Fig. 7. Structure of $[Cu_2(OOCC_6H_5)_2(dppe)_2(\mu\text{-}dppe)]\cdot 4H_2O$ (reprinted with permission from Ref. [68]; Copyright 1997 Elsevier).

Table 2
X-ray crystal structure data for Cu(I) carboxylate complexes with diphosphines

Compounds	Type of structure	Bond distances [Å]		Distance [Å]	Angles [°]		Ref.
		Cu–P	Cu–O	Cu–Cu	P–Cu–P	O–Cu–P	
$[Cu_2(dppm)_2(\mu\text{-}OOCCH_3)]BF_4{\cdot}(CH_3)_2CO$	Dinuclear (quasi-planar triangular)	2.254(2); 2.258(2); 2.241(2); 2.243(2)	2.029(4); 1.993(4)	2.7883(11)	130.56(6); 128.87(6)	115.48(12); 113.08(12); 114.41(12); 116.19(12)	[58]
$[Cu_2(OOCC_6H_5)_2(dppe)_2(\mu\text{-}dppe)]{\cdot}4H_2O$	Dinuclear (distorted tetrahedral)	2.259(1); 2.304(3); 2.276(2)	2.061(4)		89.5(1); 109.7(1); 123.4(1)	111.6(1); 111.1(1); 109.8(1)	[68]
$[Cu_2(\mu\text{-}OOCCH_3)_2dppe]$	Polymeric (distorted tetrahedral)	2.178(3); 2.157(2)	2.127(3); 2.001(2); 2.011(3); 1.994(2)	2.711(1)		122.73(1); 124.28(1); 129.93(1); 122.54(1);	[80]

3. Silver(I) carboxylate complexes

Silver carboxylates are an alternative class of precursors for silver CVD that, until very recently, appear to have been largely overlooked, though the use of acetate derivatives have been reported [11,81].

In the solid state, silver(I) carboxylates [82,83] mostly form bridged dimers as in $[Ag_2(OOCC_6H_5)_2]$ [84]; they also exhibit aggregation of these dimers into a ladder forming a polymeric network (e.g. $[Ag(OOCCF_3)]_n$ [85], $[Ag(OOCC(CH_3)_3]_n$ [86], $[AgOOC(CH_3)CC(H)CH_3]_n$ [87]. Their poor solubility and light-sensitive make their structural characterization difficult [88].

3.1. Silver(I) carboxylate complexes with tertiary phosphines

In the complex $[Ag(OOCCF_3)\{P(C_6H_4CH_2NMe_2\text{-}2)_3\}]$ [89] the trifluoroacetate anion was monodentately bonded. In this case, three-coordinated silver(I) adopted an unusual T-shaped planar geometry, defined by atoms Ag1, P1, N1 and O1 (Fig. 8). The atoms Ag1, P1 and O1 form are almost linear (174.70(7)°), whereas the silver-bonded nitrogen atom N1 is perpendicular to the O1–Ag1–P1 axis (P1–Ag1–N1, 91.42(5)°, O1–Ag1–N1, 89.78(8)°) (Fig. 8).

The coordination of $P(C_6H_4CH_2NMe_2\text{-}2)_3$ to the silver(I) center has also been confirmed by $^{31}P\{^1H\}$ NMR spectroscopy. In the ^{31}P NMR spectrum, a coupling of the phosphorus to $^{107,109}Ag$ is found at −31.9 ppm, with ^1J coupling constants of $^1J^{107}Ag^{31}P$ 511 Hz and $^1J^{109}Ag^{31}P$ 603 Hz [89].

Monodentate carboxylate ion was also noted in $[Ag(OOCC_2F_5)\{(PPh_3)_3\}]$ 0.5thf [90], $[Ag(OOCH)(PPh_3)_3]$ HCOOH [75], but in contrast to the corresponding silver(I) trifluoroacetate complex, the crystal structure of $[Ag(OOCC_2F_5)(PPh_3)_3]$ 0.5thf and $[Ag(OOCH)(PPh_3)_3]$ HCOOH exhibits tetra-coordinated Ag(I) with three crystallographically independent triphenylphosphine molecules

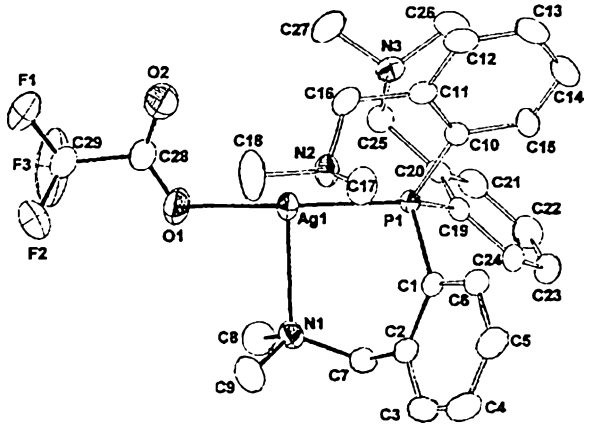

Fig. 8. Molecular geometry for $[Ag(OOCCF_3)\{P(C_6H_4CH_2NMe_2\text{-}2)_3\}]$ (reprinted with permission from Ref. [89]; Copyright 1998 Elsevier).

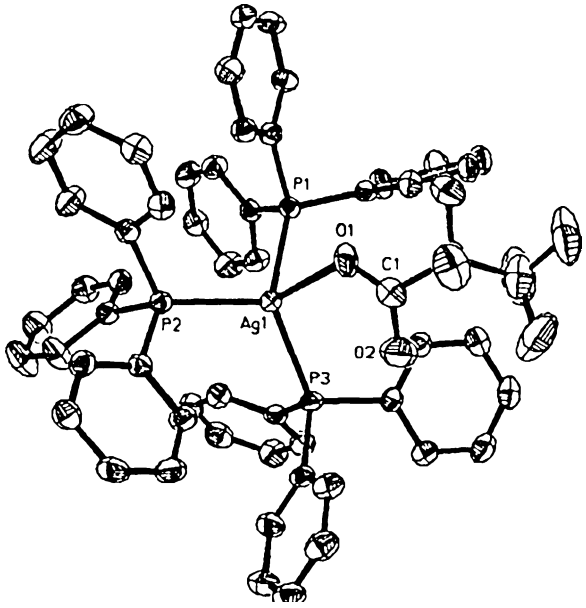

Fig. 9. Structure of $[Ag(OOCC_2F_5)\{(PPh_3)_3\}]$ (reprinted with permission from Ref. [90]; Copyright 2004 Elsevier).

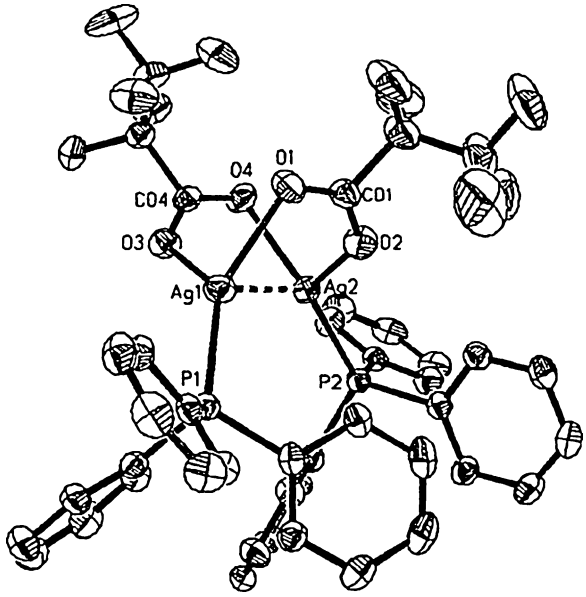

Fig. 11. Dimeric structure of $[Ag(OOCC_2F_5)(PPh_3)]_2$ (reprinted with permission from Ref. [90]; Copyright 2004 Elsevier).

occupying three coordination sites and the carboxylate anion coordinated through one oxygen atom (Fig. 9).

There are a few Ag(I) complexes with chelating carboxylate and tertiary phosphines and their X-ray crystal structure determined: $[Ag(OOCH)(2HOOCH)(PPh_3)_2]$ [91], $[Ag(OOC(CH_2)_{16}CH_3)(PPh_3)_2]$ [92], $[Ag(OOCCF_3)(PPh_3)_2]$ [93] and $[Ag(OOCC_3F_7)(PPh_3)_2]$ [94], $[Ag(OOCCH_2CN)(PPh_3)_2]$ [87], $[Ag(OOCCH_2CHCH_2CH_2)(PPh_3)_2]$ [87], $[Ag(OOC(CH_3)CHCH_3)(PPh_3)_2]$ [87].

The molecular structure of $[Ag(OOC(CH_2)_{16}CH_3)(PPh_3)_2]$ [92] contains four coordinated silver(I) with two monodentate triphenylphosphine molecules and symmetrically chelated stearate (Fig. 10). The low solubility of this species, when compared to the starting carboxylate, can be related to the long aliphatic chain and the two PPh_3 ligands, which reduces the polarity of the molecule [92].

A number of Ag(I) complexes with bridging carboxylates and tertiary phosphines have been prepared and the crystal structures of some have been determined by single crystal X-ray diffraction [35,36,90,95–98]. Dimeric structures were confirmed for $[Ag(OOCC_2F_5)(PPh_3)]_2$ [90] and $[Ag(OOCCF_3)(PCy_3)]_2$ [95] (Fig. 11), where PCy_3 and trifluoroacetate ligands were in a *syn* configuration.

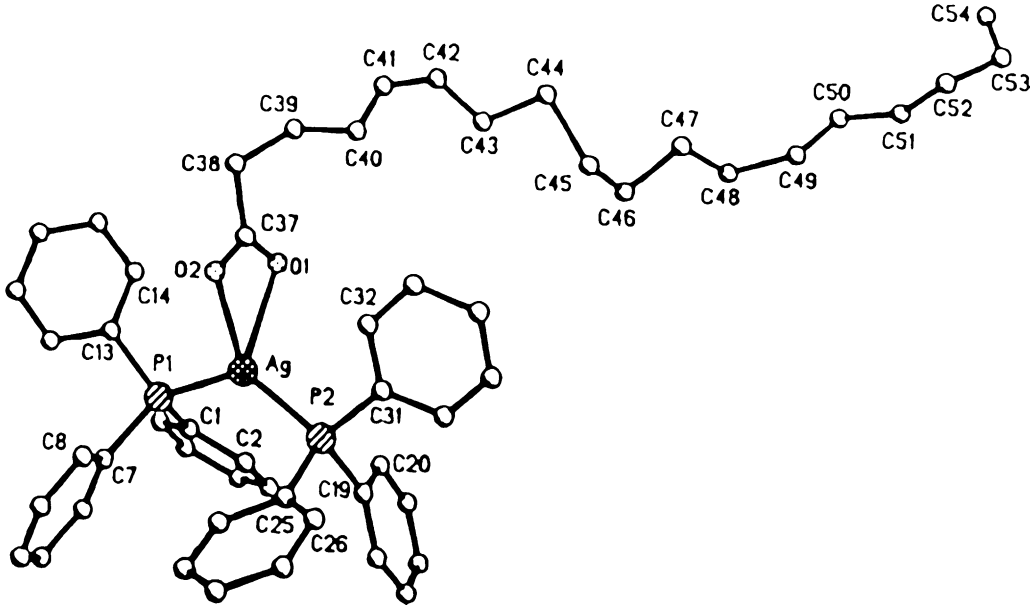

Fig. 10. Molecular structure of $[Ag(OOC(CH_2)_{16}CH_3)(PPh_3)_2]$ (reprinted with permission from Ref. [92]; Copyright 1996 Springer).

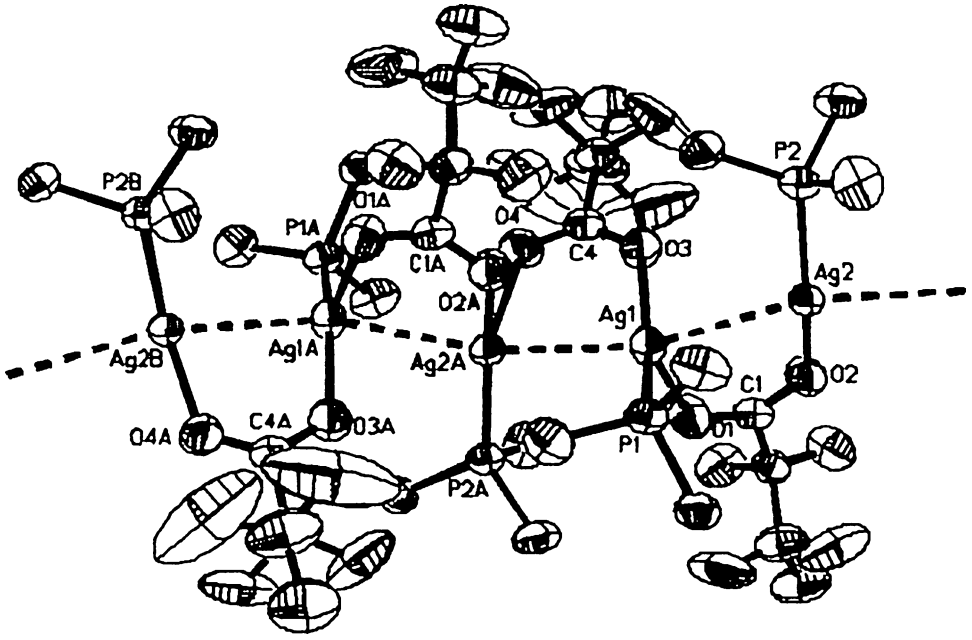

Fig. 12. Chain structure of $[Ag(OOCC_2F_5)(PMe_3)]$ (reprinted with permission from Ref. [90]; Copyright 2004 Elsevier).

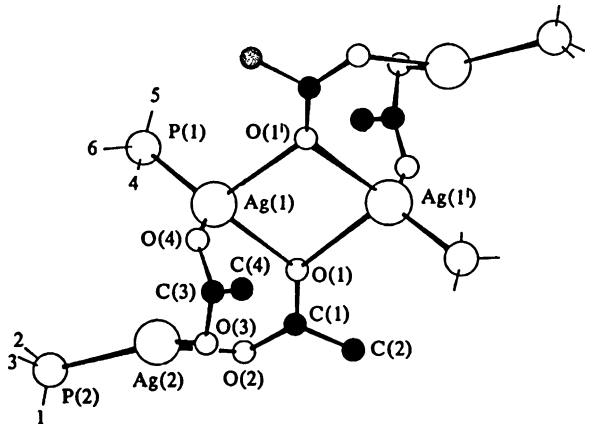

Fig. 13. Tetrameric structure of $[Ag(OOCCH_3)(PPh_3)]_4$ with phenyl rings omitted for clarity (reprinted with permission from Ref. [99]; Copyright 1977 IUCr).

Use of smaller phosphines such as PMe_3 leads to formation of a polymeric chain structure in $[Ag(OOCC_2F_5)(PMe_3)]$ [90] with bridging pentafluoropropionate and short Ag–Ag contacts holding the monomers together (Fig. 12).

The P–Ag–O and O–Ag–O angles demonstrate, that the geometry of Ag(I) is closer to T-shaped than to trigonal planar.

A special case appeared to be $[Ag(OOCCH_3)(PPh_3)]_4$ [99], were a tetrameric structure with two independent silver atoms in different environments were detected (Fig. 13).

The silver atom Ag(2) is bonded to a triphenylphosphine (Ag(2)–P(2), 2.376(3) Å) and to two oxygen atoms (Ag(2)–O(2), 2.241(8) Å, and Ag(2)–O(3), 2.260(10) Å), while the second Ag(1) is linked in a shorter distance to PPh_3 (Ag(1)–P(1), 2.354(3) Å) and to three oxygen atoms (Ag–O(4), 2.226(12) Å; Ag–O(1), 2.320(7) Å and Ag–O(1′), 2.475(7) Å) (Fig. 13) [99].

A number of silver(I) complexes with tertiary phosphines and carboxylic acid residues of general formula: $[Ag(OOCR)(PR'_3)]$, where R = CH_3, $C(CH_3)_3$, C_2F_5, C_2H_5, $(CH_3)_3SiCH_2$, C_3H_7, C_3F_7, $(CH_3)_3SiC_2H_4$, C_4H_9, C_6F_{13}, C_7F_{15}, C_8F_{17}, C_9F_{19}, C_6F_5, $C_6H_2(CH_3)_3$, R′ = Me, Et, Ph, $n = 1$, 2, were synthesized and characterized by spectroscopic methods [35–40,94]. The mode of carboxylate binding was proposed based on the COO group chemical shift in the ^{13}C NMR spectra and the splitting of the COO asymmetric and symmetric vibrations bands in the IR spectra. Relationships between the mode of carboxylate binding and COO vibrational energies are available [28]. As a criterion of carboxylate binding mode, the parameter $\Delta_{COO} = \nu_{as} - \nu_s$ (as—asymmetric, s—symmetric), is used, which is compared with the same one calculated for the respective sodium salts. Spectroscopic analysis suggest bidentate carboxylates, forming bridges between silver(I) ions [35–40,94] or in some cases a chelate mode [94].

The thermal decomposition of many Ag(I) compounds was investigated and multistage decomposition processes noted. The onset of the decomposition processes was found between 95 and 175 °C and in the first stage, detachment of the carboxylate was postulated, which was followed by dissociation of tertiary phosphine. In the case of perfluorinated carboxylates, the decomposition mechanisms are similar, but the Ag–O bond stability was lower. Thus the coordination sphere is apparently destabilized in Ag(I) carboxylates complexes with electron accepting substituents (fluorine). The Ag–O bond stability also depends on the electronic properties of the tertiary phosphines, rather than steric factors,

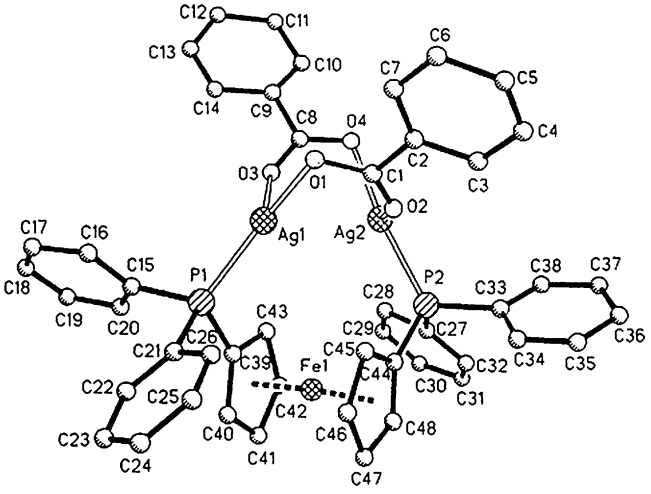

Fig. 14. Structure of $[Ag_2(\mu\text{-}OOCC_6H_5)_2(\mu\text{-dppf})]$ (reprinted with permission from Ref. [101]; Copyright 1992 ACS).

and changes in following sequence: $PMe_3 < PEt_3 < PPh_3$. The final product of the decomposition processes was metallic silver, which is evident from the analysis of TG curves and the final product powder diffractograms [100].

X-ray studies of Ag(I) complexes with phosphines and carboxylates are listed in Table 3. Many different structures are observed such as monomeric, dimeric, trimeric and polymeric, but the majority are monomeric. It is difficult to find patterns from these data but shorter aliphatic chains and perfluorinated acid residues seems to be in favour of monomeric structures. These structures are promising in future applications in CVD. The overwhelming majority of the silver atoms are four coordinate, with different degree of distortion from tetrahedral geometry. The distortion is expressed by the variances in Ag–P distances which are in the range 2.326–2.603 Å, whereas Ag–O distances are shorter being 2.173–2.533 Å, except for dimeric $[Ag(OOCC_2F_5)(PPh_3)]_2$ and monomeric $[Ag(OOCH)(PPh_3)_2]\cdot 2HCOOH$, where the Ag–O are longer (Table 3). The dimeric structures are more often observed with bulky phosphines (Pcy_3, $P(C_6H_4CH_2NMe_2\text{-}2)_3$, P^nBu_3, PPh_3).

3.2. Silver(I) carboxylate complexes with diphosphines

Diphosphines effectively stabilize Ag(I) carboxylate complexes through possible chelate and bridge binding. These ligands stabilize silver(I) in its tetrahedral and trigonal planar geometries, and influence the nuclearity of the complexes. The Ag(I) carboxylate complexes with dppf illustrate the variability of carboxylic acid residue coordination modes [101]. In $[Ag_2(\mu\text{-}OOCC_6H_5)_2(\mu\text{-dppf})]$ two trigonal planar Ag(I) ions, triply bridged by dppf (*syn*) and two benzoates were observed (Fig. 14). A similar structure was reported for $[Ag_2(\mu\text{-}OOCCF_3)_2(\mu\text{-dcpm})]$ [95].

In the case of $[Ag_4(OOCCH_3)_4(dppf)_2]$, four tetrahedral Ag(I) were interlinked by two bridging *syn*-dppf, two chelate

Table 3
X-ray crystal structure data for Ag(I) carboxylate complexes with phosphines

Compounds	Type of structure	Bond distances [Å]		Angles [°] O–Ag–P	Ref.
		Ag–P	Ag–O		
$[Ag(OOCH)(PPh_3)_3]\cdot HCOOH$ in 153 K	Monomeric	2.5199(7) 2.5237(6) 2.4953(7)	2.509(2)	89.90(7) 99.05(6) 116.10(6)	[75]
$[Ag(OOCH)(PPh_3)_3]\cdot HCOOH$ in 295 K	Monomeric	2.527(2) 2.533(2) 2.510(3)	2.507(9)	88.1(2) 99.7(2) 116.2(2)	[75]
$[Ag(OOCH)(PPh_3)_2]$	Monomeric	2.426(1)	2.425(3) 2.425(3)	112.53(9) 114.36(8)	[91]
$[Ag(OOCH)(PPh_3)_2]\cdot 2HCOOH$	Monomeric	2.426(2)	2.550(7) 2.713(8)	104.84(5) 104.26(5)	[91]
$[Ag(OOCCF_3)(Pcy_3)]_2$	Dimeric	2.377(2)	2.173(5) 2.509(6)	160.7(2)	[95]
$[Ag(OOCCF_3)\{P(C_6H_4CH_2Nme_2\text{-}2)_3\}]_4$	Tetrameric	2.3659(6)	2.183(2)	174.70(7)	[89]
$[Ag(OOCCH_3)(PPh_3)]_4$	Tetrameric	2.376(3) 2.354(3)	2.241(8) 2.260(10) 2.226(12) 2.320(7) 2.475(7)	127.7(3) 129.2(2) 128.7(2) 128.6(2)	[99]
$[Ag\{OOCC(CH_3)_3\}\{P^nBu_3\}]_2$	Dimeric	2.326(2)	2.278(4) 2.476(4)	[a]	[98]
$[Ag(OOCC_2F_5)(PPh_3)_3]\cdot 0.5thf$	Monomeric	2.6026(8) 2.5441(7) 2.5432(7)	2.433(2)	91.09(7) 107.50(6) 108.67(6)	[90]
$[Ag(OOCC_2F_5)(PPh_3)]_2$	Dimeric	2.347(1) 2.351(1)	2.212(2) 2.310(2) 2.362(2) 2.730(2)	136.87(6) 130.34(5) 150.02(6) 117.83(5)	[90]
$[Ag(OOCC_2F_5)(PMe_3)]_n$	Chain	2.343(1) 2.347(1)	2.400(3) 2.197(3) 2.194(3) 2.438(4)	113.3(1) 111.8(1) 155.6(1) 160.5(1)	[90]
$[Ag(OOCC_3F_7)(PPh_3)_2]$	Monomeric	2.430(2) 2.436(2)	2.495(5) 2.532(5)	[a]	[94]
$[Ag\{OOC(CH_2)_{16}CH_3\}(PPh_3)_2]_2$	Dimeric	2.424(3) 2.446(3)	2.399(8) 2.449(8)	114.9(2) 107.2(2) 109.5(2) 111.0(2)	[92]
$[Ag(OOCCH_2CN)(PPh_3)_2]$	Monomeric	2.419(1) 2.446(1)	2.495(2) 2.427(2)	115.66(7) 106.75(8) 124.33(6) 104.89(7)	[87]
$[Ag(OOCCH_2CHCH_2CH_2)(PPh_3)_2]$	Monomeric	2.450(2) 2.433(2)	2.401(3) 2.464(4)	107.96(10) 122.60(10) 112.49(11) 111.89(12)	[87]
$[Ag(OOC(CH_3)CHCH_3)(PPh_3)_2]$	Monomeric	2.4099(7) 2.4562(8)	2.436(2) 2.430(2)	112.16(5) 111.77(5) 121.64(5) 101.24(5)	[87]

[a] Data unavailable.

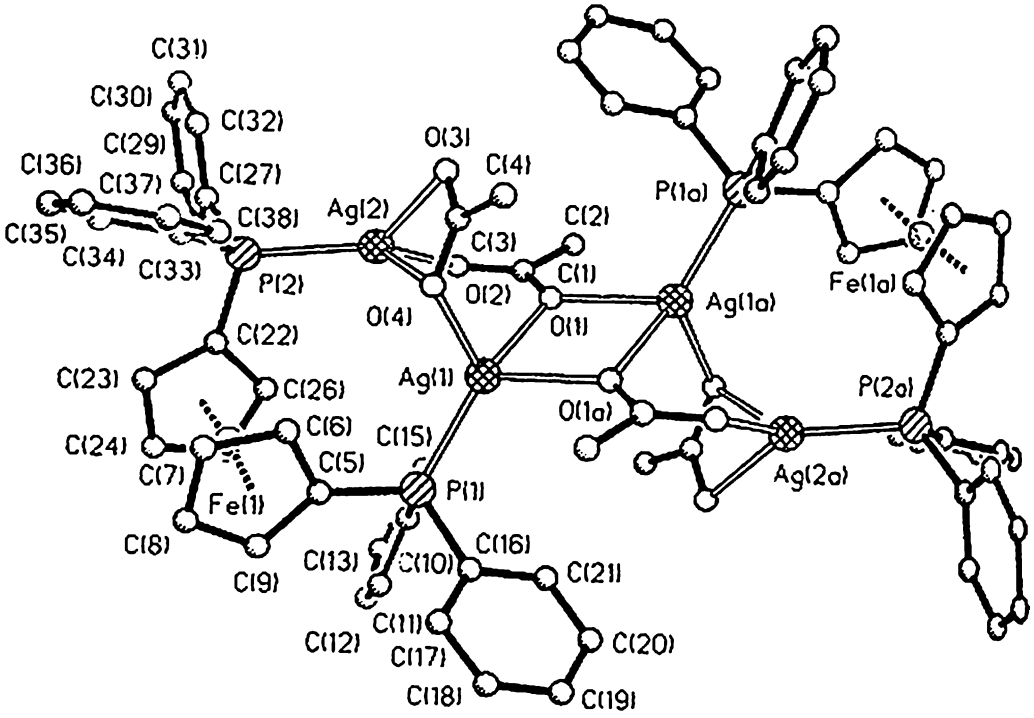

Fig. 15. Structure of $[Ag_4(OOCCH_3)_4(dppf)_2]$ (reprinted with permission from Ref. [101]; Copyright 1992 ACS).

bridging (μ_2-(η^2-O,η^1-O′)) and two triply bridging (μ_3-(η^2-O,η^1-O′)) acetates (Fig. 15). The above two complexes are examples of molecules stabilized only by bridging ligands. Moreover, VT ^{1}H and ^{31}P NMR spectra of both Ag(I)dppf compounds suggested rapid diphosphine dissociation and intermolecular exchange processes [101].

On the contrary in $([Ag_2(OOCH)_2(dppf)_3]\cdot 2CH_2Cl_2$, both monodentate formate and chelating (*syn*) and bridging (*anti*) dppf were found in a dinuclear framework (Fig. 16) [101].

The complex $[Ag_4(\mu\text{-}OOCCH_3\text{–}O,O')_2(\mu\text{-}OOCCH_3\text{–}O)_2(\mu\text{-dppm})_2]\cdot 2H_2O$ exhibited a centrosymmetric tetranuclear aggregate in the solid phase, which in solution becomes dinuclear [102,103]. The X-ray crystal structure exhibited two Ag_2 fragments linked by two acetate molecules in a monodentate mode (Fig. 17). The Ag(I) atoms in each part are bridged by dppm and acetate in an *anti–syn* fashion. This compound reacts rapidly with 2 molar equiv. of dppm to give $[Ag_2(\eta^2\text{-}OOCCH_3)_2(\mu\text{-dppm})_2]\cdot 2CHCl_3$. X-ray structural analysis of the complex confirmed its dinuclear structure, with Ag(I) atoms doubly bridged by dppm and each Ag(I) is additionally stabilized by a chelating acetate group (Fig. 18).

Complex $[Ag_2(OOCC_6H_5)_2(\mu\text{-dppm})_2]$ is dinuclear with a silver–silver distance of 3.080 Å and bridged by two dppm ligands [104]. In addition, each silver atom was coordinated by one oxygen atom from a terminal phenylacetate group. Therefore, each silver atom is in a highly distorted $AgOP_2$ trigonal planar geometry.

In solution, based on ^{31}P NMR data analysis, compounds of general formula $[Ag_2(OOCR)_2(\mu\text{-dppm})]$ and $[Ag_2(OOCR)_2\{\mu\text{-}(Ph_2P)_2CHMe\}]$, where R = CH_3, C_2H_5, *i*-C_3H_7, C_6H_5 and $[Ag_2(OOCCH_3)_2(\mu\text{-dppe})]$ exhibit dimeric structures with bridging diphosphines. The coordination around the silver atoms was completed by a carboxylate linked either in a chelating or a bridging mode [105].

Complexes of Ag(I) perfluorinated carboxylates with dppm of general formula $[Ag_2(OOCR)_2dppm]$, where R = CF_3, C_2F_5, C_3F_7, C_4F_9, C_6F_{13}, C_9F_{19}, were charac-

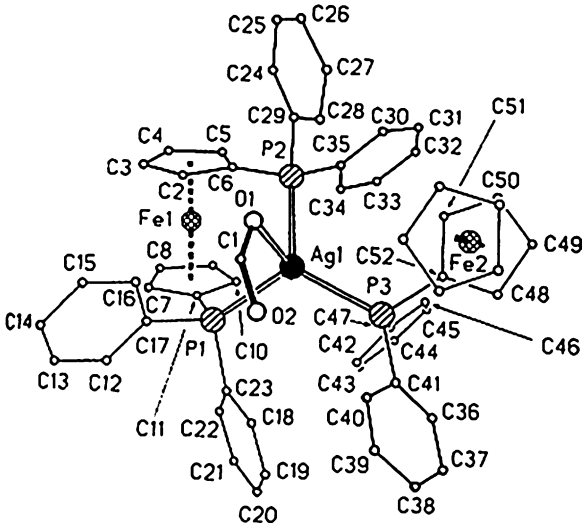

Fig. 16. Perspective view of the structure of $[Ag_2(OOCH)_2(dppf)_3]\cdot 2CH_2Cl_2$, showing half molecule, which is centrosymmetric at the atom center Ag(2) of the bridging dppf ligand (reprinted with permission from Ref. [101]; Copyright 1992 ACS).

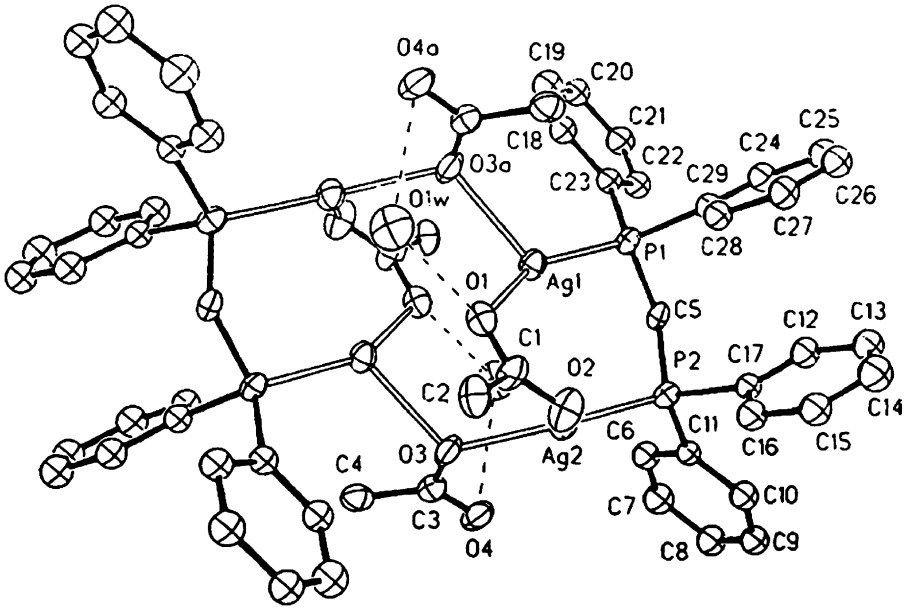

Fig. 17. Structure of $[Ag_4(\mu\text{-}OOCCH_3{-}O,O')_2(\mu\text{-}OOCCH_3{-}O)_2(\mu\text{-dppm})_2]\cdot 2H_2O$ (reprinted with permission from Ref. [102]; Copyright 1995 ACS).

terized by multinuclear NMR and IR. The X-ray structure of $[Ag_4(\mu\text{-dppm})_2(\mu\text{-}OOCC_2F_5)_4]$ exhibited the centrosymmetric tetranuclear aggregate with the silver atoms bridged by two dppm and four pentafluoropropionate units forming two monoatomic μ_2–(η^1–O) and two triple μ_3–(η^2–O, η^1–O′) bridges (Fig. 19). There are two crystallographically independent Ag(I) atoms, one has distorted tetrahedral geometry with one Ag–P bond and three Ag–O bonds, while the second one exhibits trigonal planar geometry with Ag–P and two Ag–O bonds. The ^{31}P CP MAS NMR spectra demonstrate splitting due to $^1J(^{107,109}Ag{-}^{31}P)$ and ^2J(P–P) coupling between crystallographically inequivalent phosphorus atoms and suggest an analogous tetranuclear structure in the solid state for R = C_3F_7, C_6F_{13}, C_9F_{19}. An analysis of coordination shifts and coupling constants of VT ^{31}P NMR spectra is in favour of the dimeric trigonal Ag(I) complexes with bridging carboxylates and dppm in solution [41,43].

X-ray crystal data for diphosphine silver compounds are listed in Table 4. In comparison to monophosphines more complicated di-, tetranuclear or polymeric structures are observed. The Ag–P distances are in the range 2.340–2.544 Å, whereas Ag–O are 2.182–2.840 Å. Ag–P

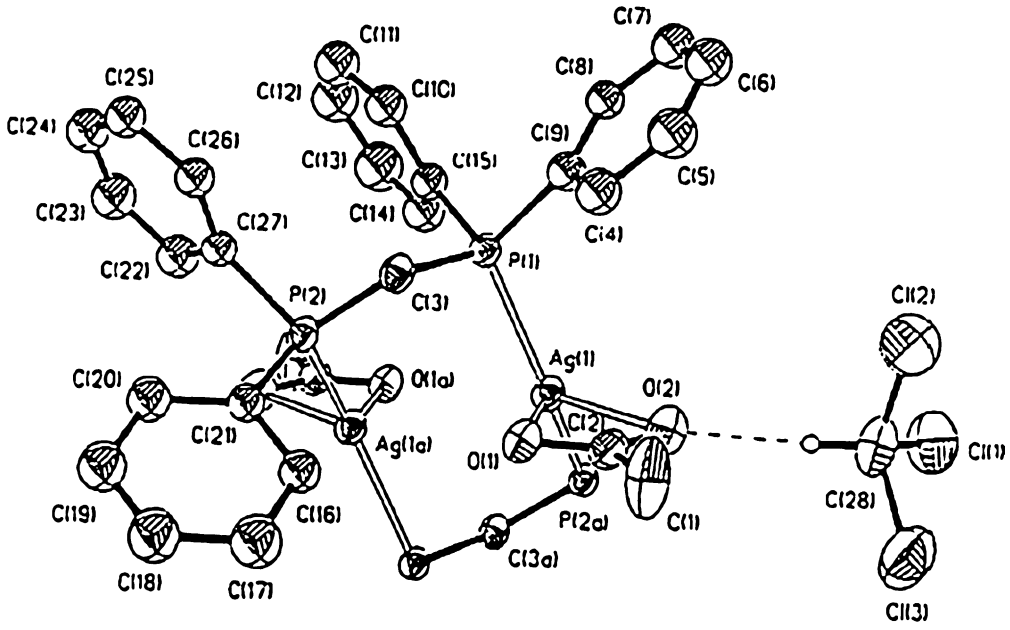

Fig. 18. Structure of $[Ag_2(\eta^2\text{-}OOCCH_3)_2(\mu\text{-dppm})_2]\cdot 2CHCl_3$ (reprinted with permission from Ref. [102]; Copyright 1995 ACS).

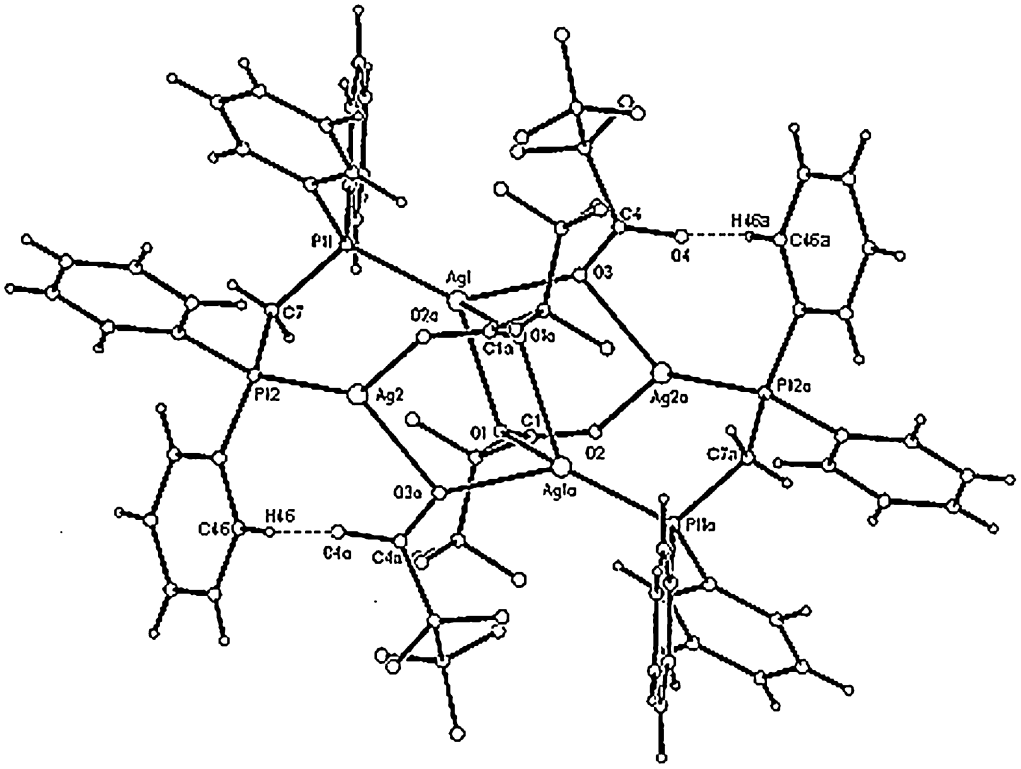

Fig. 19. $[Ag_4(\mu_2\text{-}OOCC_2F_5{-}O)_2(\mu_3\text{-}OOCC_2F_5{-}O,O,O')_2(\mu\text{-dppm})_2]$ (reprinted with permission from Ref. [41]; Copyright 2003 RSC).

bond distances are close to those observed for complexes with PR_3 whereas the Ag–O distances are slightly longer. Due to the complexicity and large molecular weight, these species are less promising CVD precursors.

4. Gold(I) complexes with carboxylates and tertiary phosphines

Volatile complexes of gold(I) appear to be less studied as CVD precursors than organometallic compounds. Well known organometallic precursors of metallic gold β-diketonates $(CH_3)_2Au$(β-diketonate), where β-diketonate = acac, tfacac, hfacac are difficult to synthesis [106,107]. Perfluorinated carboxylates or *t*-butyl derivatives of short chain carboxylates that improve the volatility of the complexes have been chosen as alternatives. However, carboxylates form a weak bond with soft gold(I) because they are σ-donors with hard oxygen donors. Therefore, the stability of the complexes has to be enhanced by σ-donor, π-acceptor ligands such as tertiary phosphines. Thus phosphine stabilized gold(I) complexes of general formula $[Au(OOCR)(PR'_3)]$ may be an alternative to organometallic CVD precursors. These complexes, besides their potential for application in CVD, [108] were studied as homogeneous catalysts [109,110] and in medicinal applications [111,112].

The synthesis of gold(I) complexes of general formulae $[Au(OOCR)(PR'_3)]$ where R′ = Me, Et, Ph, ^{p}tol and R = CH_3, $C(CH_3)_3$, $CHCl_2$, CF_3, C_3F_7, C_6F_{13}, C_7F_{15}, C_9F_{19}, C_6F_5, $C_6F_5CH_2$, $CH(CH_3)NHC(O)C_6H_5$, $CH_2NHC(O)CH_3$, $CH_2NHC(O)C_6H_5$ have been reported [44–46,113–115]. They were obtained in a metathetical reaction of (phosphine)gold(I) halide and silver carboxylates [44–46,114,115]:

$$[AuCl(PR'_3)] + AgOOCR \rightarrow [Au(OOCR)(PR'_3)] + AgCl$$

Structural studies showed these species to be monomers of type **I** (Scheme 1) or dimers of type **II** (Scheme 1) [90]. The molecular structure of gold(I) complexes depends on the steric effect of the tertiary phosphine and carboxylate substituents (e.g. $[Au(OOCCF_3)(PMe_3)]$ [116] and $[Au\{OOCC(CH_3)_3\}(PPh_3)]$ [117]).

X-ray crystal structures have been reported for some Au(I) acetate complexes: $[Au(OOCCHCl_2)(PPh_3)]$ [114] (Fig. 20), $[Au(OOCCF_3)(PPh_3)]$ [115] (Fig. 21), $[Au(OOCCH_3)(PPh_3)]$ [118] and $[Au\{OOCC(CH_3)_3\}$

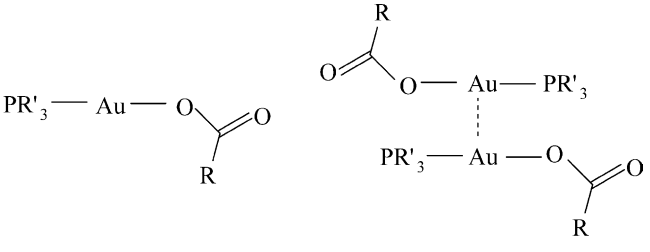

I II

Scheme 1.

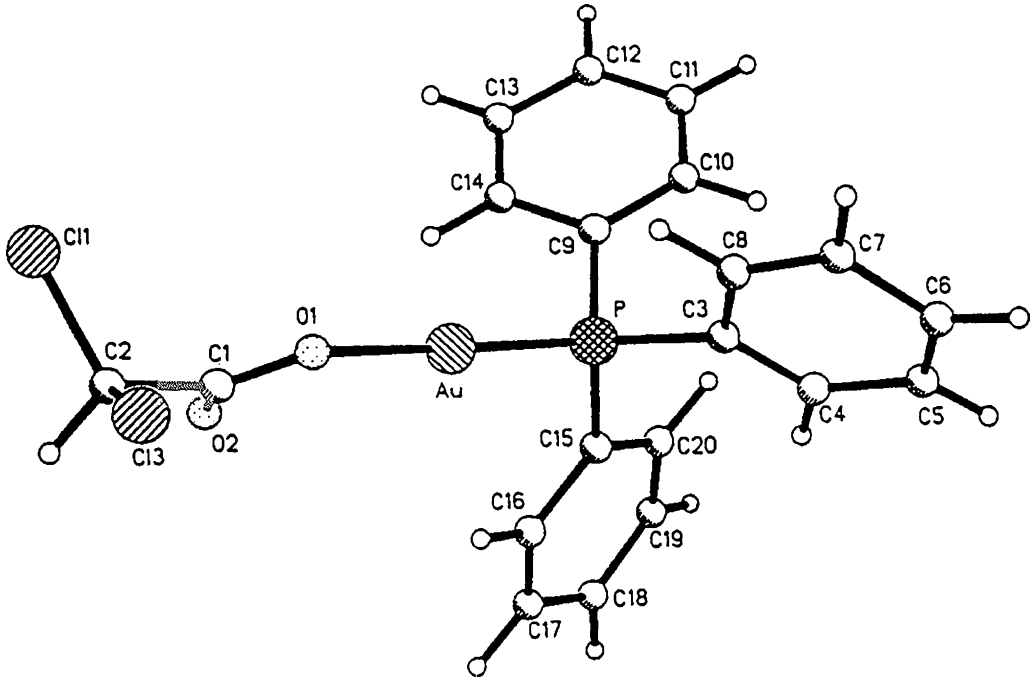

Fig. 20. Molecular structure of [Au(OOCCHCl$_2$)(PPh$_3$)] (reprinted with permission from Ref. [114]; Copyright 1995 Springer).

(PPh$_3$)] [117] which contains two independent monomers with very similar structure (Fig. 22).

The complexes crystallize as isolated monomers of type **I** (Scheme 1) [90], where each Au(I) center is linear (Table 5).

The bulkiness of phosphine and pivalate ligands prevents the close approach of the monomers, which might have allowed an auriophilic contact between the metal atoms.

In contrast, the asymmetric unit of [Au(OOCC$_2$F$_5$){P(^{p}tol)$_3$}] [117] contains only one molecule, with a close to linear P–Au–O axis (178.7(1)°). Some interesting structures

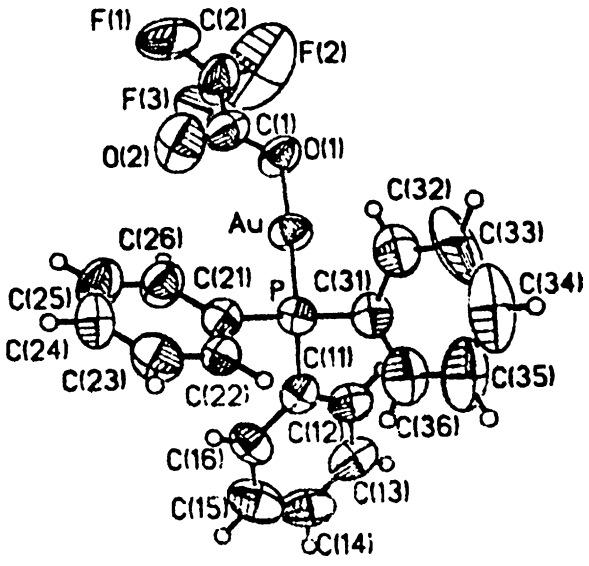

Fig. 21. A view of [Au(OOCCF$_3$)(PPh$_3$)] (reprinted with permission from Ref. [115]; Copyright 1988 IUCr).

have been reported for gold(I) complexes with triphenylphosphine and amino acid derivatives [111,112] (Fig. 23).

The coordination at gold is linear, with P–Au–O 174.6(1)°, and two molecules are linked by H bonding between N and the benzoyl O (N···O 3.00 Å) (Fig. 24).

The second type of coordination (Scheme 1) is observed with (trimethylphosphine)gold(I) trifluoroacetate (Fig. 25). which is trimeric with two short Au···Au (type **II**, Scheme 1) contacts in an angular Au···Au···Au unit [116]. These trimers are a part of spiral chains running along the *x*-axis of the crystal.

In addition the individual monomers have a typical linear configuration at the gold atoms with angles: O(11)–Au(1)–P(1), 177.0(5)°; O(21)–Au(2)–P(2), 168.9(5)°; O(31)–Au(3)–P(3), 178.9(5)° (Fig. 26).

In a search for compounds with oxygen ligands (hard donors) a series of complexes [Au(OOCR)(PR$'_3$)] involving perfluorinated carboxylates (R = C_2F_5, C_3F_7, C_6F_{13}, C_7F_{15}, C_8F_{17}, C_9F_{19}, C_6F_5, $C_6F_5CH_2$) and tertiary phosphines (R′ = Me [46], Et [45], Ph [44]) were reported. The compounds were characterized by means of multinuclear magnetic resonance (^{13}C, ^{19}F, ^{31}P), IR and thermal analysis [44–46]. The mode of carboxylate binding was derived from the analysis of chemical shift of COO group in ^{13}C NMR spectra and splitting of the COO bands (asymmetric and symmetric vibrations) using the criterion proposed by Nakamoto [28]. Evidently there is Au(I) linear coordination, with monodentately bonded tertiary phosphine and carboxylates. The tendency of gold(I) to form linear two-coordinate complexes can be explained by the large 6s → 6p energy separation caused by relativistic effects [119]. X-ray

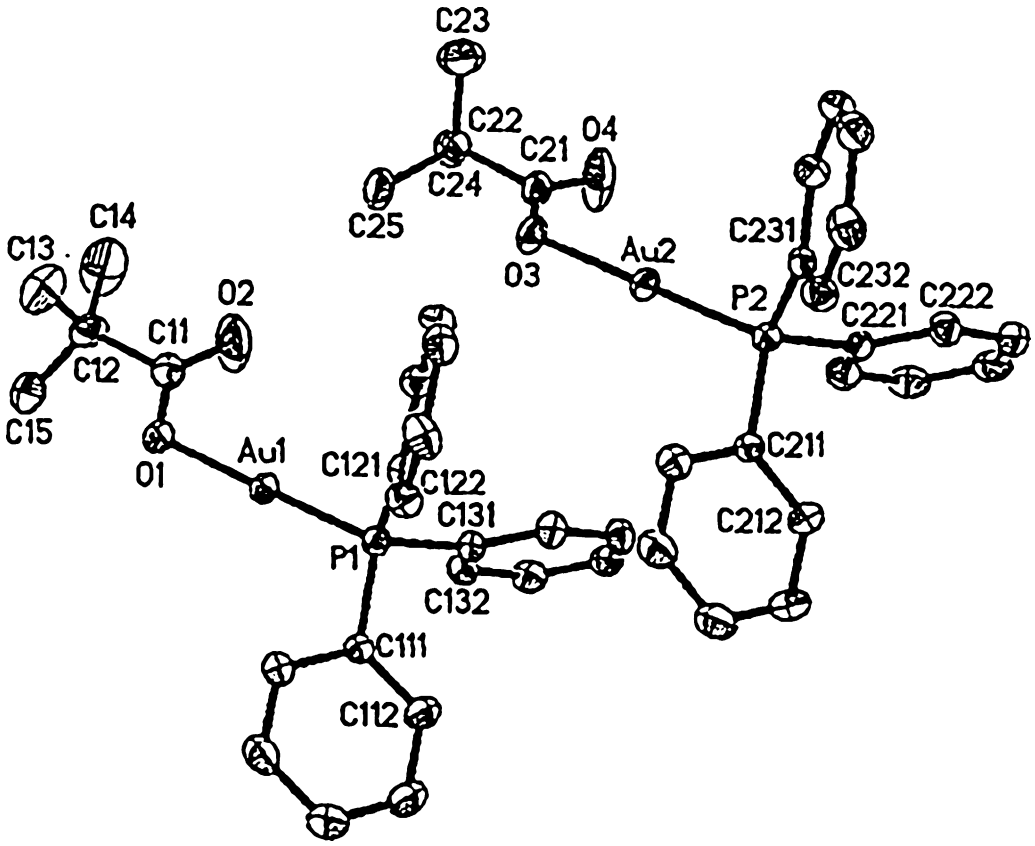

Fig. 22. The two independent molecules of [Au{OOC(CH_3)$_3$}(PPh_3)] (reprinted with permission from Ref. [117]; Copyright 2002 ZNaturforsch Muenchen).

crystal studies of Au(I) complexes with phosphine and carboxylate ligands are listed in Table 5. The structures are linear and monomeric, except for [Au($OOCCF_3$)(PMe_3)] for which a trimeric structure was detected. The largest deviations of the O–Au–P angle from linearity were observed for [Au{$OOCCH(CH_3)NHCOC_6H_5$}(PPh_3)] and [Au{$OOCC(CH_3)_3$}(PPh_3)]. The latter most probably was caused by packing forces between the large organic groups. The Au–O distances were between 2.205 and 2.224 Å, whereas Au–P distances fall in the range 2.108–2.205 Å, (Table 5) suggesting stronger Au–P bond than Au–O. The monomeric structures favour the future use of phosphine Au(I) carboxylate complexes in CVD.

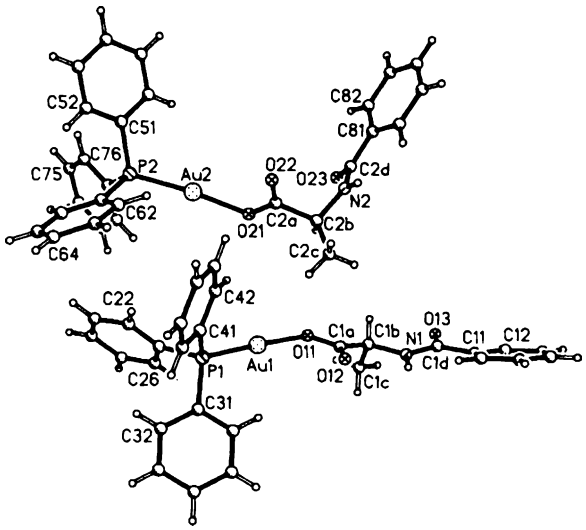

Fig. 23. The two independent molecules of triphenylphosphine-(*N*-benzyl-L-alaninato)gold(I) (reprinted with permission from Ref. [112]; Copyright 1991 Elsevier).

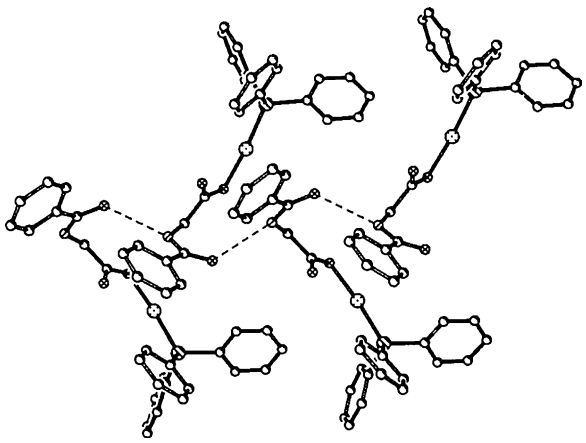

Fig. 24. The hydrogen bonds linked the molecules of triphenylphosphine-(*N*-benzyl-L-alaninato)gold(I) into chains (reprinted with permission from Ref. [112]; Copyright 1991 Elsevier).

Table 4
X-ray crystal structure data for Ag(I) carboxylate complexes with diphosphines

Compounds	Type of structure	Bond distances [Å]			Angles [°]			Ref.
		Ag—P	Ag—O	Ag—Ag	P—Ag—P	O—Ag—P	O—Ag—O	
$[Ag_4(\mu\text{-}OOCCH_3\text{—}O,O')_2(\mu\text{-}OOCCH_3\text{—}O)_2(\mu\text{-}dppm)_2]\cdot 2H_2O$	Centrosymmetric tetranuclear	2.390(4); 2.363(4)	2.485(10); 2.397(11); 2.265(11); 2.232(11)			151.6(3); 121.3(3); 115.8(3); 153.8(3)	79.9(4); 90.0(4);	[102]
$[Ag_2(\eta^2\text{-}OOCCH_3)_2(\mu\text{-}dppm)_2]\cdot 2CHCl_3$	Dinuclear	2.473(3); 2.437(3)	2.611(3); 2.547(7)	3.194(2)	146.1(1)	130.2(2); 106.7(2); 82.2(2); 102.5(2)	50.4(2)	[102]
$[Ag_4(\mu_2\text{-}OOCC_2F_5\text{-}O)_2(\mu_3\text{-}OOCC_2F_5\text{-}O,O,O')_2(\mu\text{-}dppm)_2]$	Centrosymmetric tetranuclear	2.3612(8); 2.3498(8)	2.356(2); 2.356(2); 2.485(2); 2.308(6); 2.336(2); 2.840(2)	3.8021(6); 3.0415(7); 3.9412(7); 5.9251(7)		130.88(5); 138.16(5); 127.94(5); 140.53(6)	80.92(7); 80.73(8); 76.52(7); 83.14(8)	[41]
$[Ag_2(OOCC_6F_5)_2(\mu\text{-}dppm)_2]$	Centrosymmetric dinuclear	2.429(1); 2.438(1); 2.438(1)	2.328(3)	3.080(1)	149.2(1)	107.4(1); 100.3(1)		[104]
$[Ag_2(\mu\text{-}OOCC_6H_5)_2(\mu\text{-}dppf)]$	Dinuclear	2.340(4); 2.364(5)	2.219(9); 2.182(9); 2.400(1); 2.477(8)	3.346(4)		150.9(2); 152.3(2); 107.8(3); 98.1(2)	100.7(4); 106.7(3)	[101]
$[Ag_4(OOCCH_3)_4(dppf)_2]$	Tetranuclear	2.365(2); 2.344(2)	2.298(5); 2.376(5); 2.667(5); 2.268(2); 2.393(5); 2.396(4)	3.104(1)		123.8(1); 126.5(2); 114.5(1); 98.1(2)	105.6(2); 114.1(2); 51.2(2);	[101]
$[Ag_2(OOCH)_2(dppf)_3]\cdot 2CH_2Cl_2$	Dinuclear	2.523(5); 2.496(5); 2.544(5)	2.65(2)		109.3(2); 115.0(1); 116.4(1);	89.9(3); 103.0(3); 119.8(3)		[101]
$[Ag_2(\mu\text{-}OOCCF_3)_2(\mu\text{-}dcpm)]$	Polymeric	2.354(1)	2.191(3); 2.446(4)	2.8892(9)		152.3(1); 113.5(1)		[95]

Table 5
X-ray crystal structure data for Au(I) carboxylate complexes with phosphines

Compounds	Type of structure	Bond distances [Å]		Angles [°]	Ref.
		Au—P	Au—O	O—Au—P	
$[Au(OOCCF_3)(PPh_3)]$	Monomeric	2.208(4)	2.107(8)	176.9(3)	[115]
$[Au(OOCCF_3)(PMe_3)]$	Trimeric	2.204(5); 2.217(5); 2.214(5)	2.057(14); 2.09(2); 2.08(2)	177.0(5); 168.9(5); 178.9(5)	[116]
$[Au(OOCCHCl_2)(PPh_3)]$	Monomeric	2.210(3)	2.049(9)	176.9(2)	[114]
$[Au\{OOCC(CH_3)_3\}(PPh_3)]$	Monomeric (unit contains two independent monomers)	2.217(1); 2.214(1)	2.052(3); 2.0500(3)	173.03(9); 171.82(9)	[117]
$[Au(OOCC_2F_5)\{P(^p tol)_3\}]$	Monomeric	2.204(1)	2.069(4)	178.7(1)	[117]
$[Au\{OOCCH(CH_3)NHCOC_6H_5\}(PPh_3)$	Monomeric (unit contains two independent monomers)	2.223(5)	2.069(13); 2.070(12)	177.9(4); 172.0(4)	[112]
$[Au(OOCCH_3)(PPh_3)]$	Monomeric	2.207(3)	2.063(6)	177.3(2)	[118]
$[Au\{OOCCH_2NHCOC_6H_5\}(PPh_3)$	Monomeric	2.212(2)	2.077(5)	174.6(1)	[111]

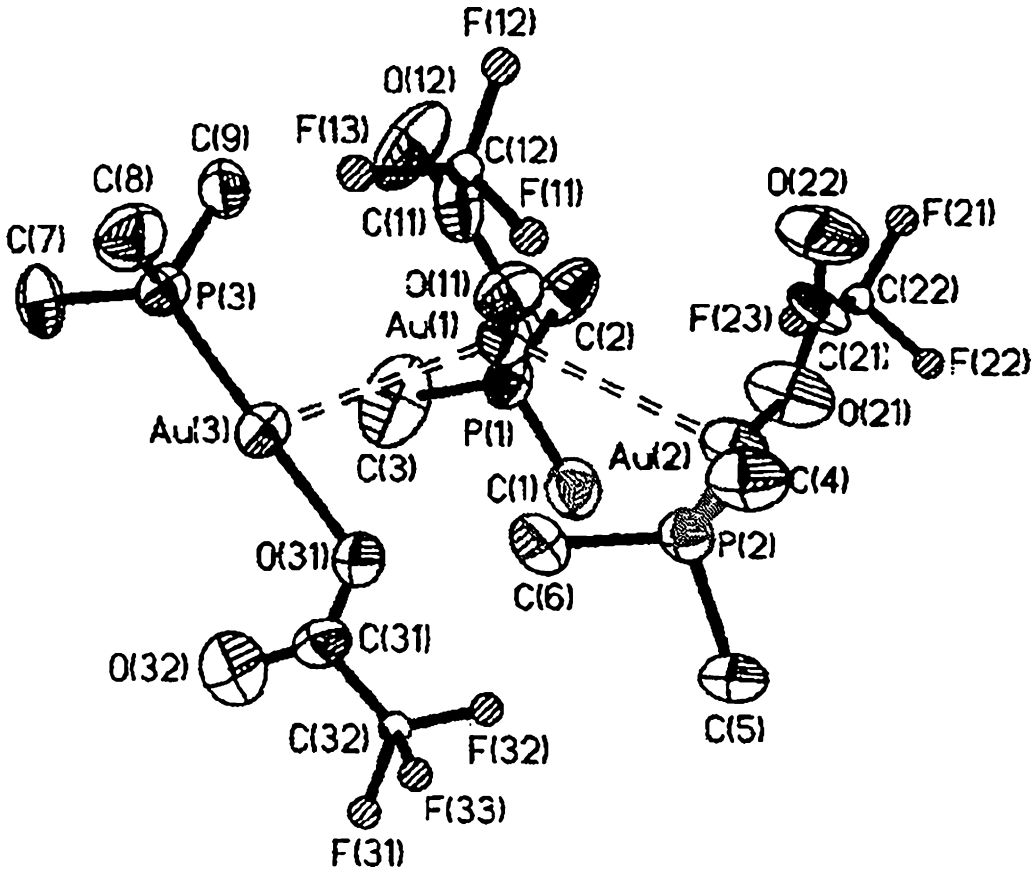

Fig. 25. Molecular structure of (trimethylphosphine)gold(I) trifluoroacetate (reprinted with permission from Ref. [116]; Copyright 1999 RSC).

5. Copper(I), silver(I) and gold(I) carboxylate derivatives as a potential chemical vapour deposition precursors for thin metallic films

Compounds used in CVD processes should have the following requirements: (a) high volatility, (b) volatile metal containing species should be stable during transport in the gas phase, (c) suitable decomposition parameters. Fluorinated and non-fluorinated metal-β-diketonates of (Cu(I), Cu(II), Ag(I), and Au(I)) stabilized by Lewis-base (L), have usually been used as CVD precursors [1,2,14–23,120–122]. Selected $[M^{(I)}(\beta\text{-diketonate})L]$ complexes parameters applied in CVD of metallic layers are listed in Table 6.

The most important CVD precursor parameters such as volatility (expressed as pressure) and deposition temperature are lower in the case of copper(I) complexes than silver(I) (Table 6). This can be connected with the stronger stabilization of Ag(I) than Cu(I) with π-donor ligands (VTMS, VTES). Having an even greater impact on deposition temperature is trimethylphosphine (strong σ-donor, weak π-acceptor), which more effectively stabilizes softer Ag(I) than Cu(I). From Table 6 it is evident, that silver deposition temperature decreases in the following order [Ag(hfac)(PMe_3)] > [Ag(hfac)(VTES)] > [Ag(hfac)(BTMSA)] caused by the differences in σ-donor, π-acceptor properties of the secondary ligands (PMe_3, VTES, and BTMSA). The π-donor

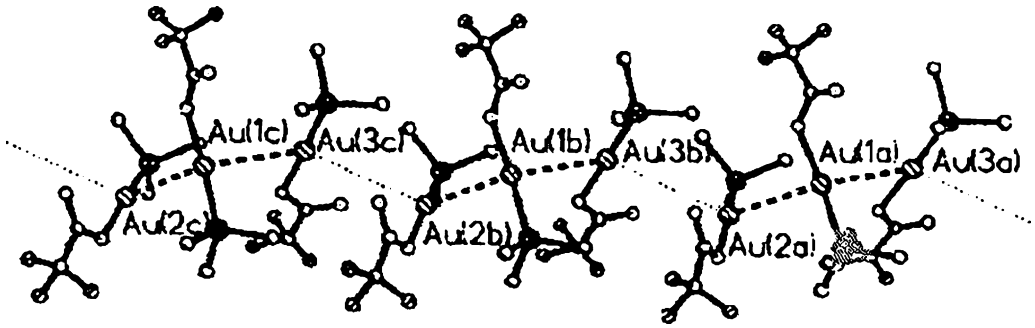

Fig. 26. Chain formation of the trimers of $[Au(OOCCF_3)(PMe_3)]$ (reprinted with permission from Ref. [116]; Copyright 1999 RSC).

Table 6
Coordination compounds used as CVD precursors of thin Cu, Ag, Au films

Precursors	Substrate	Deposition temperature T_D [°C]	Pressure [Torr]	Carrier gas	Ref.
Cu(I)					
[Cu(hfac)]	Si/SiO_2				[14]
[Cu(acen)]	Si/SiO_2				[14]
[Cu(hfac)(PMe_3)]	$Pt/W/SiO_2$	150–300	0.01	No	[18]
[Cu(tfac)(PMe_3)]	$Pt/W/SiO_2$	100–150	0.01	No	[18]
[Cu(acac)(PMe_3)]	$Pt/W/SiO_2$	<80	0.01	No	[18]
[Cu(hfac)(VTMS)]	Si/SiO_2	100–150	no	H_2/N_2	[19]
[Cu(hfac)(CO)]	Si/SiO_2				[14]
[Cu(tris(pyrazol)borates]	Glass	370–390	1.00	N_2/Ar	[20]
Cu(II)					
[Cu(acac)$_2$]	Quartz/Si/MgO/Al	145–170	21	He/H_2	[21]
[Cu(dpm)$_2$]	Quartz/Si/MgO/Al	135–155	21	He/H_2	[21]
[Cu(tfac)$_2$]	Quartz/Si/MgO/Al	85–110	21	He/H_2	[21]
[Cu(hfac)$_2$]	Quartz/Si/MgO/Al	50–60	21	He/H_2	[21]
[Cu(OCHMeCH$_2$NMe$_2$)$_2$]	Si/SiO_2	230–350	4.4×10^{-3}	N_2	[22]
[Cu(OCHMeCH$_2$NEt$_2$)$_2$]	Si/SiO_2	230-350	4.4×10^{-3}	N_2	[17]
Ag(I)					
[Ag(acac)]	Si/SiO_2	200–250		H_2	[23]
[Ag(hfac)(PMe_3)]	Glass, Si, Cu	250–450	0.05	No	[120]
[Ag(hfac)(PEt_3)]	Glass, Si, Cu	250–350	0.05	No	[20]
[Ag(fod)(PMe_3)]	Glass, Si, Cu	230-300	0.10	H_2	[20]
[Ag(fod)(PEt_3)]	Glass, Si, Cu	230–260	0.10	H_2	[20]
[Ag(hfac)(VTES)]	Si/SiO_2	160–280	0.10	No	[120]
[Ag(hfac)(BTMSA)]	Si/SiO_2	150–250	0.10	No	[16]
[Ag(hfac)(tmeda)]	Glasss	300–450		N_2/H_2	[121]
Au(I)					
[Au(hfac)(Me)$_2$]	$GaAs/SiO_2$	160–320	1.50/30.00/100.00	H_2	[2]
[Au(tfac)(Me)$_2$]	Si/SiO_2	200–300	10^{-5}	H_2	[1,122]
[Au(acac)(Me)$_2$]	Si/SiO_2	200–300	10^{-5}	H_2	[1,122]
[Au($OSiMe_3$)(Me)$_2$]$_2$	Si/SiO_2	135			[1]

properties of VTES and BTMSA cause weaker stabilization of the Ag–O bonds and reduce the deposition temperature. The Au(III) organometallic compounds are the most volatile species listed in Table 6, but the methyl group forms a covalent Au–C bond, whose nature is different from the ligands discussed above. However, their stability is comparable to silver(I) due to the effectiveness of σ Au–C bonds.

Structural parameters also have an impact on the stability of the precursors and their application in CVD methods. Clearly, a lack of intermolecular interactions has a significant impact on volatility, which is evident in the case of copper(I) and silver(I) β-diketonate precursors listed in Table 6 [18–20]. Distortion of the coordination geometry may also influence the volatility. This may be observed in the X-ray structure of [Ag(hfac)(PMe_3)] (Fig. 27) where distortion of the trigonal planarity of Ag(I) is evident [106]. This distortion alternates the bond distances and angles: (Ag–P = 2.311(3)–2.326(4) Å, Ag–O1 = 2.268(8)–2.292(8) Å, Ag–O2 = 2.297(8)–2.309(8) Å, O–Ag–P = 131.5(2)–147.7(2)°, O1–Ag–O2 = 80.0(3)–80.7(3)°). Aside from different Ag–O distances, the angles are also far away from the planar 120°, and this may cause reduction of Ag–ligand bond stability.

The deposition of pure thin metal films from these compounds arises from a thermally induced disproportionation process, which in the case of [M(β-diketonate)L] (M = Cu(I), Ag(I)) complexes can be expressed as follows: [1,15,18,20,106]

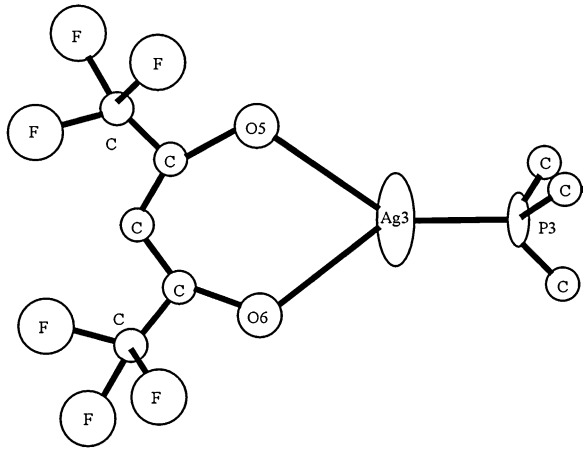

Fig. 27. View of the molecular structure of [Ag(hfac)(PMe_3)] (reprinted with permission from Ref. [106]; Copyright 1995 ACS).

Table 7
Copper(I), silver(I), and gold(I) carboxylate complexes used as CVD precursors of thin metallic films

Precursors	Method	Substrate	Deposition temperature T_D [°C]	Pressure [mbar]	Carrier gas	Detected impurities	Ref.
Cu(I)							
$[Cu_2(oxalate)L_2]$							[69]
Ag(I)							
[Ag(OOCMe)]	CVD, LICVD	Glass	380	No	No	No	[1,11]
[Ag(OOC^{t}Bu)]	CVD	Si/MgO	250–510	0.01	Ar	C, O	[17]
$[Ag(OOCCF_3)]$	CVD, LICVD	No data	600	No data	H_2	No	[1]
$[Ag(OOCC_2F_5)]$	CVD	Si/Glass	270–350	4	Ar	C, O	[125]
$[Ag(OOCC_2F_5)(PMe_3)]$	CVD	Si/Glass	210–290	4	Ar	C, O	[125]
$[Ag(OOCC_3F_7)(PMe_3)]$	CVD	Si/Glass	190–220	4	Ar	C, O, F, P	[108]
$[Ag(OOCC_8F_{17})(PMe_3)]$	CVD	Si/Glass	190–220	4	Ar	C, O, F	[108]
$[Ag\{OOCC(CH_3)_3\}(PMe_3)]$	CVD	Si	180–200	2–4	Ar	C, O	[126]
$[Ag\{OOCC(CH_3)_3\}(PEt_3)]$	CVD	Si	180–200	2–4	Ar	C, O	[126]
$[Ag\{OOCC(CH_3)_3\}(P^nBu_3)]$	CVD	$Si/LaAlO_3$	>540	10	N_2		[17]
$[Ag\{OOCC(CH_3)_3\}(PMe_3)_2]$	AACVD	Glass	310	1000	N_2	C, P	[94]
$[Ag\{OOCC(CH_3)_3\}(PPh_3)_2]$	AACVD	Glass	310	1000	N_2	C	[94]
$[Ag(OOCC_4H_7)(PPh_3)_2]$	AACVD	Glass	300	1000	N_2	C, O	[87]
$[Ag(OOC(Me)C{=}C(H)Me)(PPh_3)_2]$	AACVD	Glass	200–348	1000	N_2	C, O, P	[87]
$[Ag(OOCC_2H_2Ph)(PPh_3)_2]$	AACVD	Glass	200–398	1000	N_2	C, O	[87]
$[Ag(OOCCF_3)(P^nBu_3)_2]$	CVD	SiO_2	300–350	1–50	N_2	No data	[127,128]
Au(I)							
$[Au(OOCC_3F_7)(PEt_3)]$	CVD	Si/Glass	260–290	4	Ar	C, O, F	[108]
$[Au(OOCC_7F_{15})(PMe_3)]$	CVD	Si/Glass	260–290	4	Ar	C, O, F	[108]

$$2[Cu^{(I)}(\beta\text{-diketonate})L] \rightarrow Cu^0 + [Cu^{(II)}(\beta\text{-diketonate})_2] + 2L \quad (1)$$

These precursors have low thermal stability and are air and moisture sensitive which is a problem for their use in CVD. In spite of that, classical vapourization methods are ineffective and the CVD requires special deposition techniques, e.g. low-pressure [106], pulsed-laser [122] photo-assisted decomposition [123] or a special precursor delivery systems [120,124].

The advantages of metal carboxylate derivatives over β-diketonates, appears to be: simpler synthesis, lower moisture sensitivity, and sufficient thermal stability. Silver(I) carboxylates and their complexes with tertiary phosphines were successfully used in CVD methods and results are listed in Table 7.

The structural parameters of complexes listed in Tables 1–5 will now be discussed with relation to their applications in CVD methods.

5.1. Metal carboxylate as potential CVD precursors

The air and moisture instability of copper(I) and gold(I) carboxylates makes them less useful in CVD experiments, however, volatility studies of these compounds have been reported [29]. For example, copper(I) formate and acetate were readily sublimed between 160 and 180 °C in vacuo [48,49]. Mass spectrometry studies of [Cu(OOCR)] (R = H, Me, Bu^t, CF_3, C_2H_3, C_3H_5, Ph) [129] showed that aliphatic carboxylates were stable and sublimed without decomposition, forming in the gas phase, copper containing fragments $[Cu_2(OOCR)]^+$, $[Cu_2(OOCR)_2]^+$, $[Cu_2(OOCR)(OOC)]^+$. In the case of the unsaturated carboxylates, which are thermally unstable and decompose during sublimation, the organometallic fragments: CuR_2, Cu_2R_2, Cu_2R and copper(I) carboxylate species: $[Cu_2(OOCR)]^+$, $[Cu_2(OOCR)_2]^+$, $[Cu_2(OOCR)(R)]^+$) were detected. Ogura and Fernando suggested that dimeric copper(I) patterns, transported in the gas phase, can form four types of structures (Fig. 28), which can be identified by gas-phase IR spectroscopy [129].

The relatively low volatility and thermal stability of silver(I) acetate and trifluoroacetate [130] requires, for conventional CVD methods, heating between 250 and 600 °C and pressure 0.10–0.01 mbar. However, pure silver films (100% Ag, 0% C) were deposited from silver(I) acetate and triflu-

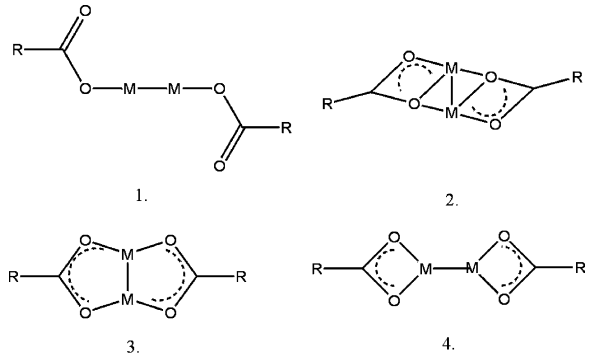

Fig. 28. The possible dimeric structures for the Cu(I) carboxylates transported in vapours (reprinted with permission from Ref. [129]; Copyright 1973 ACS).

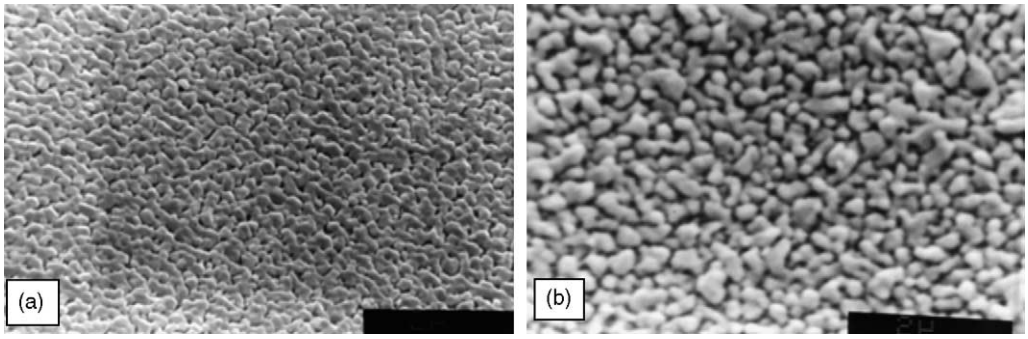

Fig. 29. Scanning electron micrographs of silver films deposited from [Ag(OOCC$_2$F$_5$)] at (a) T_D = 290 °C, XPS—79.8 Ag, 6.2% C [at.%], (b) T_D = 300 °C, XPS—78.4 Ag, 8.6% C [at.%] (*hot wall* CVD, T_V = 180 °C, Ar, p = 4 mbar) (reprinted with permission from Ref. [125]; Copyright 2001 VCH/Wiley).

oroacetate using the laser-induced CVD (LICVD) method [1]. The trifluoroacetate was heated to 60 °C, until the concentration of volatile silver species was sufficient, then, the metallic film was deposited by laser-induced pyrolysis. These promising CVD results have developed an interest in silver(I) carboxylates as a new group of metal precursors. Silver(I) trimethylacetate requires a relatively high sublimation temperature (230–510 °C under 0.01 mbar) and gives a low yield in the CVD process (≤0.2% at temperatures above 540 °C). This result can most probably be related to the polymeric chains in this compound which require a high sublimation temperature [17,86]. This compound was also examined in the aerosol-assisted CVD (AACVD) process, but due to the low solubility in organic solvents, the application of this method was troublesome.

Conventional thermal CVD method (*hot-wall* CVD) has also been used for the deposition of thin silver films from [Ag(OOCR)] (R = C_2H_5, C_2F_5, C_3F_7), though promising results were obtained only for [Ag(OOCC$_2$F$_5$)] [125,132]. Metallic layers (Fig. 29) were deposited at 290 °C, in Ar atmosphere, pressure: 4 mbar, on Si(1 1 1) and glass substrates.

The volatility of selected Ag(I) carboxylates, and the stability of silver containing species transported in vapours were studied using MS and variable temperature IR methods [17,86,131,132]. As with the Cu(I) carboxylates, the principal main signals were attributed to $[Ag_2(OOCR)]^+$, $[Ag_2(OOCR)(OOC)]^+$, $[Ag_2(OOCR)_2]^+$ (Table 8). Their stability depends on the length of aliphatic chain (C_xH_{2x+1} or C_xF_{2x+1}), or the presence of hydrocarbon groups with quaternary carbon –C(Me)$_3$). Only for R = CH_3/CF_3, C_2H_5/C_2F_5, C_3H_7, and C(Me)$_3$, the volatility of the dinuclear silver species is suitable for transport in the gas phase. However [Ag(OOCR)] (R = C_2H_5 and C_3F_7) completely decompose during the sublimation.

Considering the MS data, the following fragmentation mechanism has been proposed: [17,132]

$$2[Ag(OOCR)]\,(s) \rightarrow [Ag_2(OOCR)_2]\,(g) \quad (2)$$

$$[Ag_2(OOCR)_2]\,(g) \rightarrow Ag^0\,(s) + AgR\,(g) + OOCR^*\,(g) + CO_2\,(g) \quad (3)$$

According to this scheme, sublimation of silver carboxylates (Eq. (2)) is followed by thermal decomposition (Eq. (3)) [17]. Results for [Ag(OOCC$_2$F$_5$)] revealed that while the thermal stability of these volatile dinuclear silver species may be suitable for their transport in the gas phase, another decomposition mechanism may occur (Eq. (4)) [127]:

$$2[Ag(OOCC_2F_5)] \rightarrow 2Ag + C_4F_{10} + 2CO_2 \quad (4)$$

Variable temperature IR studies were carried out over a heated precursor surface with silver(I) pentafluoropropionate. The IR spectra showed the formation of species containing coordinated carboxylate groups between 200 and 270 °C [132]. The absorption band from coordinated carboxylate groups

Table 8
Mass spectra of selected silver carboxylates [Ag(OOCR)] (including the main dinuclear Ag(I) species) [131,132]

R	CH_3		C_2H_5		C_3H_7		C_5H_{11}		C_7H_{15}		C_9H_{19}		$C_{11}H_{23}$		$C(CH_3)_3$	
	m/z	%	*m/z*	%	*m/z*	%	*m/z*	%	*m/z*	%	*m/z*	%	*m/z*	%	*m/z*	%
$[Ag_2(O_2CR)]^+$	273	12.8	287	152.0	301	42.4	329	11.6	357	6.5	385	2.9	413	2.2	315	16.9
$[Ag_2(O_2CR)(O_2C)]^+$	317	1.1	331	4.7	345	0.4	–	–	–	–	–	–	–	–	–	–
$[Ag_2(O_2CR)_2]^+$	332	0.5	360	0.5	388	0.1	–	–	–	–	–	–	–	–	–	–

	CF_3		C_2F_5		C_3F_7	
	m/z	%	*m/z*	%	*m/z*	%
$[Ag_2(O_2CR)]^+$	327	48.2	379	10.0	429	3.9
$[Ag_2R]^+$	–	–	209	34	–	–

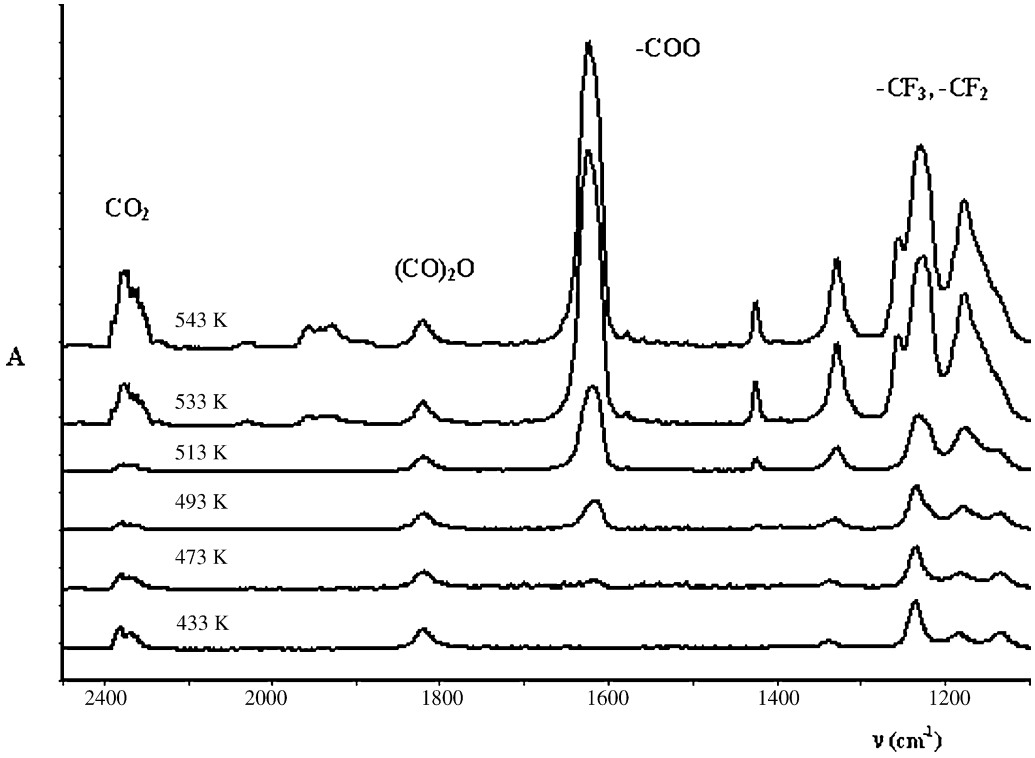

Fig. 30. Temperature variable IR spectra of vapours formed during the pyrolysis of [Ag($OOCC_2F_5$)] (KBr, $p = 10^{-1}$ mbar, Ar).

(1606 cm^{-1}) was detected in IR spectra of vapours transported with a carrier gas, between 220 and 270 °C (Fig. 30). Because the intensity of this band increases with temperature, the concentration of Ag–OOC fragments in vapour at higher temperatures was evidently greater. These results were in good agreement with *hot-wall* CVD experiments, and suggested that the properties of [Ag($OOCC_2F_5$)] are suitable for use as a silver precursor. Concluding, one can propose the presence of silver containing species while being transported in the gas phase as presented in Eq. (3).

5.2. Cu(I), Ag(I), and Au(I) carboxylate complexes with tertiary phosphines as CVD precursors

Silver(I) carboxylate complexes with tertiary phosphines have, so far, been more intensively studied as precursors for CVD studied than copper(I) and gold(I) analogs (Table 7) [17,87,94,108,125–128]. Crystallographic data on (phosphine)silver(I) carboxylates ([Ag($OOCR'$)(PR_3)$_i$] ($R' = C_nF_{2n+1}$, $C(CH_3)_3$, R = Me, Et, i = 1–3), Table 3, Figs. 9–13) demonstrate that they form at least four types of structures. When complexes with diphosphines (Table 3) are considered, even more structural variations are possible. Therefore, these structural parameters may have significant impact on the CVD parameters in contrast to the [Ag(β-diketonate)(PR_3)] complexes which are mostly monomeric (Fig. 27) [106,133]. For β-diketonate complexes, the stabilisation of the coordination sphere seems to be a more important feature than the type of molecular structure.

The bis-triphenylphosphine Ag(I) carboxylate complexes are monomeric, and based on their similar spectroscopic properties [94], similar structures can be proposed for trimethyl-, triethyl- and tributylphosphine silver(I) complexes of general formula ([Ag($OOCR'$)(PR_3)$_2$], R = Me, Ph, $R' = C_4H_7$, C_2H_2Ph, $C(CH_3)_3$). The low thermal stability of bis-phosphine adducts (monomeric structures) in the gas phase caused, these silver compounds to be used mainly in the AACVD techniques [94]. However, [Ag($OOCCF_3$)(PBu_3^n)$_2$] also exhibits promising properties as a Ag precursor in thermally induced CVD methods [128]. The Ag–P bond distances in monomeric, chain or dimeric structure are longer than the Ag–O bond distances. This can be a reason for the low thermal stability of species transported in the gas phase and necessity of AACVD technique application, for the monomeric precursors. Bis-phosphine monomeric precursors exhibited a higher deposition temperature (T_D = 300–350 °C) for metallic films production than analogous trimethylphosphine and tributylphosphine adducts (T_D between 210 and 290 °C, Table 7). To explain the differences between these precursors, variable temperature MS studies of the latter have been carried out [127]. Analysis of spectra recorded in the range 120–220 °C, exhibited signals from phosphine fragmentation (m/z = 202 PBu^n). In the spectrum recorded at 230 °C, silver containing fragments were noticed at m/z = 309 ([$AgPBu^n$]$^+$), 511 ([Ag(PBu^n)$_2$]$^+$), and

527 ($[OAg(PBu^n)_2]^+$ or $[Ag(PBu^n)(OPBu^n)]$). Considering these data, the following decomposition mechanism was proposed:

$$[Ag(OOCR)(PBu_3{}^n)_2] \xrightarrow{120-220\,^\circ C} 2PBu_3{}^n + [Ag(OOCR)] \quad (5)$$

$$[Ag(OOCR)(PBu_3{}^n)2] \xrightarrow{290\,^\circ C} [Ag(PBu_3{}^n)n] + {}^*OOCR \quad (6)$$

where R = CF_3, C_2F_5, n = 1, 2.

Accordingly, volatile phosphorus by-products, condensed during the CVD process may be a source of undesired contaminants of these metallic films.

There are other reports on the application of Ag(I) carboxylate trimethyl- or triethylphosphines in CVD techniques, where decomposition process pathways, different from those described above, were presented [107,125,126]. Silver layers were deposited at lower temperatures (T_D = 190–290 °C, p = 4 mbar) for $[Ag(OOCR)(PMe_3)]$ (R = C_2F_5, C_3F_7, C_8F_{17}), and (T_D = 180–200 °C, p = 2–4 mbar) for $[Ag(OOCBu^t)(PR'_3)]$ (R′ = Me, Et). Metallic films were free from phosphorus impurities, but contaminated with carbon and oxygen, which was evident from XPS. The phosphorus contamination was explained by VT-MS studies of $[Ag(OOCC(CH_3)_3)(PR'_3)]$ (R′ = Me, Et), recorded between 80 and 260 °C. Lines from phosphorus fragments were detected, such as PMe_3, m/z = 76, PEt_3 m/z = 118, and $[Ag(PEt_3)]$ m/z = 225, which were the main species in the gas phase. The diagrams presented in Fig. 31 show $[Ag(PEt_3)]$ m/z = 225 (18%), as a predominant fragment, whereas in the case of trimethylphosphine the intensity of $[Ag(PMe_3)]$ m/z = 183, was less than 2%. However at higher temperatures (160–260 °C), the main fragment appears to be $[Ag_2(O_2CC(CH_3)_3)]^+$ (m/z = 317).

When MS data were compared with the X-ray crystal structures of silver(I) carboxylate complexes with tertiary phosphines [90,94], the influence of molecular structure on decomposition pathway becomes evident. The species $[Ag_2(OOCR)_2(PMe_3)_2]$ (R = C_2F_5, $C(CH_3)_3$) involves dimers forming a chain structure, with three-coordinated silver atoms, bridged by the carboxylate ligands and short silver–silver contacts [94]. The dimers were not detected in complexes with more than one phosphine molecule per metal atom, as for $[Ag_2(OOCCF_3)_2(PBu_3{}^n)_4]$ [90]. Therefore, the thermal stability of complexes with a chain structure was different from complexes whose structures do not consists of dimers e.g. $([Ag_2(OOCR)_2(PR'_3)_2]_n)$. MS studies of $[Ag_2(OOCC(CH_3)_3)_2(PMe_3)_2]_n$ (chain structure) demonstrate detachment of PMe_3 between 80 and 140 °C and formation of the solid silver(I) carboxylate derivatives. In the same temperature range, the decomposition of $[Ag_2(OOCC(CH_3)_3)_2(PEt_3)_2]_n$ (liquid, non associated dimers) proceeds with formation of a volatile silver–phosphine species. The second step of thermal decomposition (160–260 °C), of both types of complexes, can be related to the detachment of a volatile silver–carboxylate species.

The different stabilities of the silver containing species, transported in the gas phase, is the main factor influencing the structure and quality of the deposited layers. Triphenylphosphine complexes were also used in CVD experiments [94] but silver layers demonstrated much worse parameters when compared with trimethylphosphine or triethylphosphine adducts.

Carbon impurities were detected, by X-ray photoelectron spectroscopy (XPS) and energy-dispersive X-ray spectroscopy (EDXS) in silver films grown from (phosphine)silver(I) carboxylates on Si, or glass substrates (Table 7). Moreover, oxygen and traces of fluorine impurities were detected in some films (Table 7). Trace amounts of phosphorus were found in layers fabricated from $[Ag(OOCC(CH_3)_3)(PMe_3)_2]$, $[Ag(OOCC_3F_7)(PMe_3)]$, and $[Ag(OOC(Me)C{=}C(H)Me)(PPh_3)_2]$, which can be related to the stable $[AgPR_n]$ species detected in the gas phase.

Deposition rates for precursor used in AACVD methods varied between 1.4 and 2.6 nm min^{-1} [87,94] and were higher than for films fabricated by thermally induced CVD from $[Ag(OOCC_2F_5)(PMe_3)]$ (0.5–0.9 nm min^{-1}) [125], and $[Ag(OOCC(CH_3)_3)(PR_3)]$, R = Me, Et (1.2–1.7 nm min^{-1})

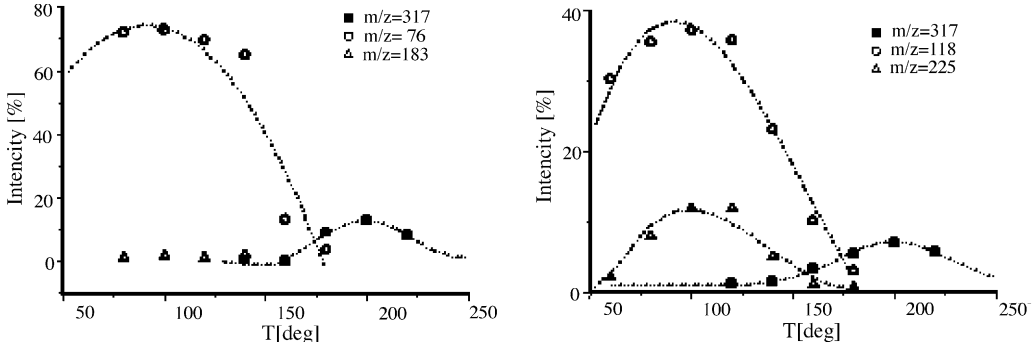

Fig. 31. The temperature evolution of the selected peaks intensity in MS spectra (EI 70 eV) of $[Ag_2(OOCC(CH_3)_3)_2(PMe_3)_2]$ (m/z = 317 ($[Ag_2(OOCC(CH_3)_3)]$, m/z = 76 ($[PMe_3]$, m/z = 183 ($[Ag(PMe_3)]$), and $[Ag_2(OOCC(CH_3)_3)_2(PEt_3)_2]$ (m/z = 317 ($[Ag_2(OOCC(CH_3)_3)]$, m/z = 118 ($[PEt_3]$, m/z = 225 ($[Ag(PEt_3)]$) (reprinted with permission from Ref. [126]; Copyright 2005 VCH/Wiley).

Table 9
Morphology of silver layers deposited from silver(I) carboxylate complexes with tertiary phosphines

Precursor	Visual appearances	Film morphology	Ref.
$[Ag(OOCC_2F_5)(PMe_3)]$	Thick white film	Smooth surface, dense packed grains	[125]
$[Ag(OOCC_3F_7)(PMe_3)]$	Thick white film	Rough surface	[108]
$[Ag(OOCC_8F_{17})(PMe_3)]$	Thick white film	Rough surface	[108]
$[Ag(OOCC(CH_3)_3)(PMe_3)]$	Silver refractive film	Rough surface, dense packed grains	[126]
$[Ag(OOCC(CH_3)_3)(PEt_3)]$	Silver refractive film	Smooth surface, dense packed grains	[126]
$[Ag(OOCC(CH_3)_3)(PMe_3)_2]$	Thick whitish film, grey partially	Dense matt crystals	[90]
$[Ag(OOCC(CH_3)_3)(PPh_3)_2]$	Silver refractive film, partially transparent	Very smooth film	[90]
$[Ag(OOCC_4H_7)(PPh_3)_2]$	Transparent silver refractive film	Smooth surface	[87]
$[Ag(OOC(Me)C{=}C(H)Me)(PPh_3)_2]$	Thin yellow film on glass, silver on the top of the plate	Uneven surface	[87]
$[Ag(OOCC_2H_2Ph)(PPh_3)_2]$	Transparent thin brown film	–	[87]
$[Ag(OOCCF_3)(PBu^n{}_3)_2]$	Thin, matt grey film	Rough surface	[127,128]

[126]. Morphology studies (SEM–scanning electron microscopy) of films deposited from (phosphine)silver(I) carboxylates using CVD and AACVD are listed in Table 9.

There appears to be no significant impact of the precursor crystal structure and silver films morphology. However, the differences between films deposited from perfluorinated and aliphatic carboxylates complexes, e.g. $[Ag(OOCC_2F_5)(PMe_3)]$ and $[Ag(OOCC(CH_3)_3)(PMe_3)]$, can be noted. The surfaces of silver films deposited from [Ag(OOCC2F5)(PMe_3)] were clear and smoother than those fabricated from $[Ag(OOCC(CH_3)_3)(PMe_3)]$ (Fig. 32). This effect may be explained the influence of carboxylate ligand on volatility and deposition precursor parameters.

Gold(I) alkyl phosphine complexes are good precursors for the CVD of gold, however their low deposition rates are a significant disadvantage [134]. Gold(I) alkyloxyphosphine compounds also exhibited excellent properties as precursors (Table 6) [135]. Gold(I) carboxylate complexes with tertiary phosphines demonstrate similar type of structures as discussed above for Ag(I) compounds, hence one may expect that these compounds can be promising precursors in CVD. The thermal decomposition of these gold complexes proceeds in a two stages process, which can be separated or coincide with each other, resulting in formation of metallic gold. For the majority of complexes, the first process appeared to be decarboxylation, which started between 140 and 160 °C, depending on the carboxylate [44]. However, there is no distinct relationship between the decarboxylation onset temperature and the length of the perfluorinated chain [44–46]. When the decarboxylation onset temperature is related to the type of phosphine, the following order is evident: $PMe_3 < PEt_3 < PPh_3$. Because the first stage is connected with breaking of the Au–O bond and detachment of carboxylate, the electronic and steric properties of the tertiary phosphines should have a noticeable impact on the thermal stability of these complexes. Stronger stabilization of the Au–O bonds arises from the presence of stronger π-acceptor ligands such as PPh_3. A hard base, such as oxygen in perfluorinated carboxylates, when linked with soft acid—gold(I), results in an excellent leaving group and minimum contamination in the metal layers. The lowest temperature of gold formation was found for $[Au(OOCC_7F_{15})(PMe_3)]$ and $[Au(OOCC_3F_7)(PEt_3)]$ (220 °C), while the highest was for $[Au(OOCC_6F_5CH_2)(PPh_3)]$ (600 °C [44–46]). Analysis of TG data suggests that the thermal stability of the selected gold(I) complexes can be acceptable for *hot-wall* CVD experiments [108]. The results obtained for $[Au(OOCC_3F_7)(PEt_3)]$ and $[Au(OOCC_7F_{15})(PMe_3)]$ are in favour of the above assumption, because dense metallic layers (Fig. 33) were produced between 260 and 290 °C ($p = 4$ mbar), on Si(1 1 1), glass, and glass fibre substrates [108].

When considering the application of copper(I) carboxylate complexes with tertiary phosphines as CVD precursors the main obstacle appeared to be their air and moisture sensitiv-

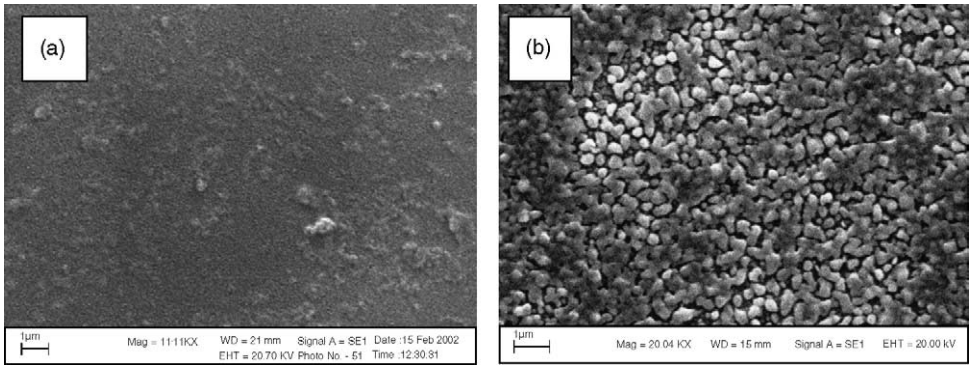

Fig. 32. Scanning electron micrographs of silver films deposited from (a) $[Ag(OOCC_2F_5)(PMe_3)]$ at $T_D = 250$ °C and (b) $[Ag(OOCC(CH_3)_3)(PMe_3)]$ $T_D = 190$ °C, (*hot wall* CVD, $T_V = 180$ °C, Ar, $p = 4$ mbar).

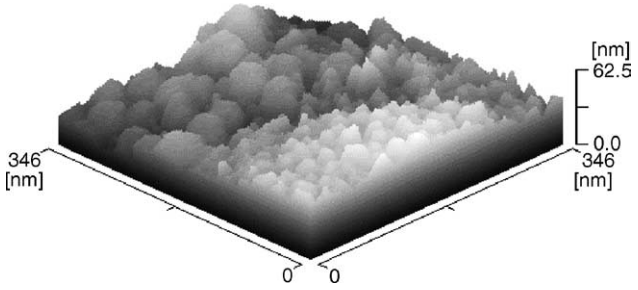

Fig. 33. Scanning tunneling electrochemical micrographs of gold film on Si(1 1 1) deposited from [Au(OOCC$_7$F$_{15}$)(PMe$_3$)], at T_D = 210 °C (reprinted with permission from Ref. [108]; Copyright 2000 VCH/Wiley).

ity. Thermal analyses, MS and temperature variable IR [29] indicates that [Cu(OOCR)(POMe$_3$)$_2$] (R = CF$_3$, C$_2$F$_5$, C$_3$F$_7$, C$_6$F$_{13}$, C$_7$F$_{15}$, C$_8$F$_{18}$, C$_9$F$_{19}$) can be useful in the preparation of Cu or Cu$_2$O layers. However, the results of CVD experiments were negative. Kohler et al. reported interesting results for the thermal behaviour of dicopper(I) oxalate complexes [69] [Cu$_2$(oxalate)L$_2$], L = Me$_3$SiC≡CSiMe$_3$, Me$_3$SiC≡CSiBu$^t_3$, Et$_2$C=CEt$_2$, H$_2$C=C(H)SiMe$_2$, which can be used in the CVD of copper layers. These compounds decomposed completely between 50 and 350 °C, to metallic copper, CO$_2$, and volatile alkyne and alkene ligands.

6. Conclusions

Cu(I) carboxylate complexes with phosphines and a monodentate carboxylate usually have a distorted tetrahedral geometry. Bidentately-linked carboxylates resulted in dimeric structures, with metal ions in trigonal geometry. In the case of complexes with alkylphosphite (R′ = Me, Et, Bu) the dimeric structure was broken apart in the solution. Silver(I) and gold(I) complexes of general formula [M(OOCR)(PR′$_3$)], where R = CH$_3$, C(CH$_3$)$_3$, C$_2$F$_5$, C$_2$H$_5$, (CH$_3$)$_3$SiCH$_2$, C$_3$H$_7$, C$_3$F$_7$, (CH$_3$)$_3$SiC$_2$H$_4$, C$_4$H$_9$, C$_6$F$_{13}$, C$_7$F$_{15}$, C$_8$F$_{17}$, C$_9$F$_{19}$, C$_6$F$_5$, C$_6$H$_2$(CH$_3$)$_3$, R′ = Me, Et, Ph, n = 1, 2 were characterized by spectroscopic methods. Spectroscopic analysis suggests bidentate carboxylates, forming bridges between silver(I) ions or in some cases, adopting a chelate mode. Thermal decomposition of Ag(I) complexes proceeds in a multistage process. The Ag–O bond thermal stability depends on the electronic properties of the tertiary phosphines, rather than the steric factors and changes in the following sequence: Me$_3$P < Et$_3$P < Ph$_3$P. Decomposition depends on the carboxylate, but there is no distinct relationship between decarboxylation temperature and the length of the perfluorinated chain. The thermal stability of complexes with a chain structure was different from dimeric complexes. Gold and silver formation temperatures detected for the complexes are acceptable for CVD hot wall experiments. Spectroscopic results suggest Au(I) in linear coordination, with monodentately bonded tertiary phosphine and carboxylates.

The air and moisture instability of copper(I) and gold(I) carboxylates makes them less useful in CVD experiments, however. MS studies showed that aliphatic carboxylates were stable and sublime without decomposition, forming silver or copper containing fragments: [M$_2$(OOCR)]$^+$, [M$_2$(OOCR)$_2$]$^+$, [M$_2$(OOCR)(OOC)]$^+$ in the gas phase. Their stability depends on the length of the aliphatic chain (C$_x$H$_{2x+1}$ or C$_x$F$_{2x+1}$), or the presence of hydrocarbon groups with quaternary carbon—C(Me)$_3$. In the case of the unsaturated carboxylates, which are thermally unstable and decompose during sublimation, organometallic fragments: CuR$_2$, Cu$_2$R$_2$, Cu$_2$R were detected.

In conclusion, the presence of stable, volatile metallated species is essential for the effective transport and metal layer formation in CVD. Morphology studies exhibited the formation of dense Ag films with the grain size between 50 and 100 nm. By varying the stability of the metal containing species, transported in the gas phase, one may influence the structure and quality of the deposited layers.

Acknowledgements

We thank the Polish State Committee for Scientific Research for grant 4T08C 039 23.

Appendix A. Abbreviations

AACVD	Aerosol-assisted chemical vapour deposition
acac	Acetylacetonato
acen	4,4′-(1.2-Ethanediyldinitrilo)bis(2-pentadionato)
BTMSA	Bis(trimethylsilyl)acetylene
CPTOSSB	Cross polarization total sideband suppression B
Cy	Cyclohexyl
CVD	Chemical vapour deposition
dcpm	Bis(dicyclohexylphosphino)methane
dpm	2,2,6,6-Tetramethyl-3,5-heptanedionato
dppf	1,1′-Bis(diphenylphosphino)ferrocene
dppm	Bis(diphenylphosphino)methane
dppe	Bis(diphenylphosphino)ethane
Et	Ethyl
etp$_3$	1,1,1-Tris((diphenylphosphino)ethyl)ethane
fod	2,2-Dimethyl-6,6,7,7,8,8,8-heptafluoro-3,5-octanedionato
hfa	Bis-hexafluoroacetylacetonate
hfac	1,1,1,5,5,5-Hexafluoroacetylacetonato
i-Bu	*iso*-Butyl
LICVD	Laser induced chemical vapour deposition
n-Bu	*n*-Butyl
Me	Methyl
m-tol	*m*-Tolyl
n-Pr	*n*-Propyl
i-Pr	*iso*-Propyl
o-tol	*o*-Tolyl
Ph	Phenyl
p-tol	*p*-Tolyl
t-Bu	*t*-Butyl
tfa	Tetraflurotoacetylacetonate
tfac	Trifluoroacetylacetonate
tmeda	*N*, *N*, *N*′, *N*′-tetramethylethylenediamine
VTES	Vinyltriethylsilane
VTMS	Vinyltrimethylsilane

References

[1] T.T. Kodas, M.J. Hampden-Smith, The Chemistry of Metal CVD, VCH, Weinheim, 1994.
[2] M. Hoshino, K. Kasai, J. Komeno, Jpn. J. Appl. Phys. 31 (1992) 4403.
[3] S.P. Murarka, Mater. Sci. Eng. 19 (1997) 76.
[4] C.L. Haynes, R.P. van Duyne, J. Phys. Chem. B 105 (2001) 5599.
[5] A. Masten, M. Brüggemann, P. Wißmann, Fresenius J. Anal. Chem. 365 (1999) 227.
[6] K. Baba, K. Yamaki, M. Miyagi, Appl. Opt. 38 (1999) 2564.
[7] R. Kalyanaraman, S. Oktyabrsky, J. Narayan, J. Appl. Phys. 85 (1999) 6636.
[8] X. Qin, W. Zhang, L. Zhang, D. Jiang, X.J. Liu, D. Jin, Phys. Rev. B 17 (1999) 2891.
[9] Y. Yonezawa, A. Takami, T. Sato, K. Yamamoto, T. Sasanuma, H. Ishida, A. Ishitani, J. Apply. Phys. 68 (1990) 1297.
[10] J. Uchil, K. Mohan Rao, M. Pattabi, J. Phys. D: Appl. Phys. 29 (1996) 2992.
[11] Y.-F. Lu, M. Takai, T. Shiokawa, Y. Aoyagi, J. Appl. Phys. 33 (1994) 1313.
[12] R.J.H. Voorhoeve, J. Merewether, J. Electrochem. Soc. 119 (1972) 364.
[13] M.J. Shapiro, W.J. Lackey, J.A. Hanigofsky, D.N. Hill, W.B. Carter, E.K. Barefield, J. Alloys Compd. 187 (1992) 331.
[14] M.J. Hampden-Smith, T.T. Kodas, Chem. Vap. Deposition 1 (1995) 8.
[15] P. Doppelt, Coord. Chem. Rev. 178–180 (1998) 1785.
[16] K.-M. Chi, Y.-H. Lu, Chem. Vap. Deposition 7 (2001) 117.
[17] S. Samoilenkov, M. Stefan, G. Wahl, S. Paramanov, N. Kuzmina, A. Kaul, Chem. Vap. Deposition 8 (2002) 74.
[18] H.K. Shin, K.M. Chi, M.J. Hamoden-Smith, T.T. Kodas, J.D. Farr, M. Paffett, Chem. Mater. 4 (1992) 788.
[19] M.L.H. ter Heerdt, P.J. van der Put, J. Schoonaman, Chem. Vap. Deposition 7 (2001) 199.
[20] C. Pettinari, F. Marchetti, C. Santini, R. Pettinari, A. Drozdov, S. Troyanov, G.A. Battiston, R. Gerbasi, Inorg. Chim. Acta 315 (2001) 88.
[21] T. Gerfin, M. Becht, K.-H. Dahmen, Mater. Sci. Eng. B17 (1993) 97.
[22] R. Becker, A. Devi, J. Weiß, U. Weckenmann, M. Winter, C. Kiener, H.-W. Becker, R.A. Fischer, Chem. Vap. Deposition 9 (2003) 149.
[23] M. Kuwarbara, N. Kusaka, Jpn. J. Appl. Phys. 27 (1988) 1504.
[24] F.A. Cotton, G. Wilkinson, Advanced Inorganic Chemistry, John Wiley and Sons, New York, 1988, p. 64.
[25] C.A. Tolman, Chem. Rev. 77 (1977) 313.
[26] D.F. Shriver, P.W. Atkins, C.H. Langford, Inorganic Chemistry, Oxford University Press, Oxford, 1994, p. 46, 212.
[27] N.N. Greenwood, A. Earnshaw, Chemistry of The Elements, Pergamon Press, Oxford, 1986, p. 1371.
[28] G.B. Deacon, R.J. Phillips, Coord. Chem. Rev. 33 (1980) 227.
[29] I. Szymańska, E. Szłyk, Materials Science 21 (2003) 245.
[30] E. Szłyk, I. Szymańska, Polyhedron 18 (1999) 2941.
[31] E. Szłyk, I. Szymańska, I. Łakomska, R. Kucharek, Annals of the Polish, Chemical Society, 2001, p. 177.
[32] R. Kucharek, E. Szłyk, I. Szymańska, Polish J. Chem. 75 (2001) 337.
[33] R. Kucharek, E. Szłyk, I. Szymańska, J. Coord. Chem. 53 (2001) 55.
[34] E. Szłyk, R. Kucharek, I. Szymańska, L. Pazderski, Polyhedron 22 (2003) 3389.
[35] I. Łakomska, A. Grodzicki, E. Szłyk, Thermochim. Acta 303 (1997) 41.
[36] I. Łakomska, E. Szłyk, A. Grodzicki, Thermochim. Acta 315 (1998) 121.
[37] E. Szłyk, I. Łakomska, A. Surdykowski, A. Goliński, Polish J. Chem. 73 (1999) 1763.
[38] E. Szłyk, I. Łakomska, Polish J. Chem. 76 (2002) 1399.
[39] E. Szłyk, I. Łakomska, A. Grodzicki, Polish J. Chem. 68 (1994) 1529.
[40] E. Szłyk, I. Szymańska, R. Szczęsny, Annals of the Polish, Chemical Society, 2003, p. 507.
[41] E. Szłyk, I. Szymańska, A. Surdykowski, T. Głowiak, A. Wojtczak, A. Goliński, J. Chem. Soc. Dalton Trans. (2003) 3404.
[42] E. Szłyk, I. Szymańska, P. Piszczek, A. Goliński, M. Chaberski, Progr. Coord. Bioinorg. Chem. (2003) 343.
[43] E. Szłyk, A. Goliński, Polish J. Chem. 74 (2000) 895.
[44] E. Szłyk, I. Łakomska, A. Grodzicki, Polish J. Chem. 69 (1995) 1103.
[45] E. Szłyk, I. Łakomska, A. Grodzicki, Current Trends in Coordination Chemistry, Slovak Technical University Press, Bratislava, 1995, p. 151.
[46] I. Łakomska, A. Grodzicki, E. Szłyk, Polish J. Chem. 72 (1998) 492.
[47] M.G.B. Drew, D.A. Edwards, R. Richards, J. Chem. Soc. Dalton Trans. (1977) 299.
[48] M.G.B. Drew, D.A. Edwards, R. Richards, J. Chem. Soc. Chem. Commun. (1973) 124.
[49] D.A. Edwards, R. Richards, J. Chem. Soc. Dalton Trans. (1973) 2464.
[50] T.P. Lockhart, D.A. Haitko, Polyhedron 4 (1985) 1745.
[51] P.F. Rodesiler, E.L. Amma, J. Chem. Soc. Chem. Commun. 4 (1974) 599.
[52] R.D. Mounts, T. Ogura, Q. Fernando, Inorg. Chem. 13 (1974) 802.
[53] A. Toth, C. Floriani, A. Chiesi-Villa, C. Guastini, Inorg. Chem. 26 (1987) 236.
[54] F.A. Cotton, E.V. Dikarev, M.A. Petrukhina, Inorg. Chem. 39 (2000) 6072.
[55] J.A. Connor, A.C. Jones, R. Price, J. Chem. Soc. Chem. Commun. 4 (1980) 137.
[56] J.A. Connor, D. Dubowski, A.C. Jones, J. Chem. Soc. Perkin Trans. 1 5 (1982) 1143.
[57] R.L. Beddoes, J.A. Connor, D. Dubowski, A.C. Jones, O.S. Mills, J. Chem. Soc. Dalton Trans. 10 (1981) 2119.
[58] P.D. Harvey, M. Drouin, T. Zhang, Inorg. Chem. 36 (1997) 4998.
[59] D.J. Darensbourg, E.M. Longridge, M.W. Holtcamp, K.K. Klausmeyer, J.H. Reibenspies, J. Am. Chem. Soc. 115 (1993) 8839.
[60] N. Marsich, A. Camus, G. Nardin, J. Organomet. Chem. 239 (1982) 429.
[61] D.J. Darensbourg, M.W. Holtcamp, E.M. Longridge, K.K. Klausmeyer, J.H. Reibenspies, Inorg. Chim. Acta 227 (1994) 223.
[62] A. Miyashita, A. Yamamoto, J. Organomet. Chem. 113 (1976) 187.
[63] M. Dines, Inorg. Chem. 11 (1972) 2949.
[64] D.J. Darensbourg, D.L. Larkins, J.H. Reibenspies, Inorg. Chem. 37 (1998) 6125.
[65] D.J. Darensbourg, M.W. Holtcamp, E.M. Longridge, K.K. Klausmeyer, J.H. Reibenspies, J. Am. Chem. Soc 117 (1995) 318.
[66] C. Bianchini, C.A. Ghilardi, A. Meli, S. Midollini, A. Orlandini, Inorg. Chem. 24 (1985) 924.
[67] S. Kitagawa, M. Kondo, S. Kawata, S. Wada, M. Maekawa, M. Munakata, Inorg. Chem. 34 (1995) 1455.
[68] M. Biagini-Cingi, A.M. Manotti-Lanfredi, F. Ugozzoli, A. Camus, N. Marsich, Inorg. Chim. Acta 262 (1997) 69.
[69] K. Kohler, J.E.F. Meyer, D. Vidovic, Organometallics 22 (2003) 4426.
[70] D.A. Edwards, R. Richards, J. Chem. Soc. Dalton Trans. (1975) 637.
[71] R.B. Hart, P.C. Healy, G.A. Hope, D.W. Turner, A.H. White, J. Chem. Soc. Dalton Trans. 5 (1994) 773.
[72] S.J. Lippard, G.J. Palenik, Inorg. Chem. 10 (1971) 1322.
[73] M.G.B. Drew, A.H. Othman, D.A. Edwards, R. Richards, Acta Crystallogr., Sect. B (1975) 2695.

[74] D.A. Edwards, R. Richards, Spectrochim. Acta 34A (1976) 167.
[75] G.A. Bowmaker, Effendy, J.V. Hanna, P.C. Healy, J.C. Reid, C.E.F. Rickard, A.H. White, J. Chem. Soc. Dalton Trans. (2000) 753.
[76] E. Szłyk, A. Grodzicki, I. Szymańska, G. Wrzeszcz, F. Rozpłoch, Polish J. Chem. 71 (1997) 320.
[77] E. Szłyk, I. Szymańska, G. Wrzeszcz, F. Rozpłoch, Polish J. Chem. 74 (2000) 909.
[78] E. Szłyk, I. Szymańska, R. Kucharek, G. Wrzeszcz, F. Rozpłoch, Polish J. Chem. 75 (2001) 215.
[79] J. Diez, P. Gamasa, J. Gimeno, M. Lanfranchi, A. Tirpicchio, J. Chem. Soc. Dalton Trans. 3 (1990) 1027.
[80] D.J. Darensbourg, E.M. Longridge, B. Khandelwal, J.H. Reinbenspies, J. Coord. Chem. 32 (1994) 27.
[81] Y. Lu, M. Takai, S. Nagamoto, K. Kato, S. Namba, Appl. Phys. A—Mater. Sci. Process. 54 (1992) 51.
[82] P. Coggon, A.T. McPhail, J. Chem. Soc. Chem. Commun. (1972) 91.
[83] A.E. Blakeslee, J.L. Hoard, J. Am. Chem. Soc. 78 (1956) 3029.
[84] B.T. Usubaliev, E.M. Movsumov, I.R. Amiraslanov, A.I. Akhmedov, A.A. Musaev, Zh. Strukt. Khim. 22 (1981) 98.
[85] R.G. Griffin, J.D. Ellett, M. Mehrng, J.G. Bullitt, J.S. Waugh, J. Chem. Phys. 57 (1972) 2147.
[86] N. Kuzmina, S. Paramonov, R. Ivanov, V. Kezko, K. Polamo, S. Troyanov, J. Phys. IV 9 (1999) 8.
[87] D.A. Edwards, M.F. Mahon, K.C. Molloy, V. Ogrodnik, J. Mater. Chem. 13 (2003) 563.
[88] R.J. Lancashire, in: G. Wilkinson, R.D. Gillard, J.A. McCleverty (Eds.), Comprehensive Coordination Chemistry, vol. 5, Pergamon Press, Oxford, 1987, p. 808, Chapter 54.
[89] H. Lang, M. Leschke, G. Rheinwald, M. Melter, Inorg. Chem. Commun. 1 (1998) 254.
[90] P. Römbke, A. Schier, H. Schmidbaur, S. Cronje, H. Raubenheimer, Inorg. Chim. Acta 357 (2004) 235.
[91] G.A. Bowmaker, Effendy, J.V. Hanna, P.C. Healy, G.J. Millar, B.W. Skelton, A.H. White, J. Phys. Chem. 99 (1995) 3909.
[92] D.R. Whitcomb, R.D. Rogers, J. Chem. Crystall. 26 (1996) 99.
[93] S. Weng Ng, Acta Crystallogr., Sect. C Cryst. Struct. Commun. 54 (1998) 743.
[94] D.A. Edwards, R.M. Harker, M.F. Mahon, K.C. Molloy, Inorg. Chim. Acta 328 (2002) 144.
[95] Ch. Che, M. Tse, M.C.W. Chan, K. Cheung, D. Phillips, K. Leung, J. Am. Chem. Soc. 122 (2000) 2464.
[96] C. Oldham, W.F. Sandford, J. Chem. Soc., Dalton Trans. (1977) 2068.
[97] R.G. Goel, P. Pilon, Inorg. Chem. 17 (1978) 2876.
[98] S.E. Paramanov, N.P. Kuzmina, S.I. Troyanov, Polyhedron 22 (2003) 837.
[99] E.T. Blues, M.G.B. Drew, B. Femi-Onadeko, Acta Cryst. B33 (1977) 3965.
[100] Powder Diffraction File, Sets 4-783, International Centere for Diffraction Data (JCPDS) USA, 1977.
[101] T.S.A. Hor, S.P. Neo, C.S. Tan, T.C.W. Mak, K.W.P. Leung, R.J. Wang, Inorg. Chem. 31 (1992) 4510.
[102] S.P. Neo, Z.Y. Zhou, T.C.W. Mak, T.S.A. Hor, Inorg. Chem. 34 (1995) 520.
[103] A.F.M.J. van der Ploeg, G. van Koten, Inorg. Chim. Acta 51 (1981) 225.
[104] M. Hong, D. Wu, H. Liu, T.C.W. Mak, Z. Zhou, D. Wu, S. Li, Polyhedron 16 (1997) 1957.
[105] A.F.M.J. van der Ploeg, G. van Koten, A.L. Spek, Inorg. Chem. 18 (1979) 1052.
[106] Z. Yuan, N.H. Dryden, J.J. Vittal, R.J. Puddephat, Chem. Mater. 7 (1995) 1696.
[107] S. Serhini-Monim, Z. Yuan, K. Griffiths, P.R. Norton, R.J. Puddephat, J. Am. Chem. Soc. 117 (1995) 4030.
[108] E. Szłyk, P. Piszczek, I. Łakomska, A. Grodzicki, J. Szatkowski, Chem. Vap. Deposition 6 (2000) 105.
[109] M. Haruta, S. Tsubata, T. Kobayashi, H. Kugeyama, M.J. Genet, B. Delman, J. Catal. 144 (1993) 175.
[110] J.H. Teles, S. Brode, M. Chabanas, Angew. Chem. 110 (1998) 1475.
[111] P.G. Jones, R. Schelbach, J. Chem. Soc., Chem. Commun. (1988) 1338.
[112] P.G. Jones, R. Schelbach, Inorg. Chim. Acta 182 (1991) 239.
[113] Ch.M. Mitchell, F.G.A. Stone, J. Chem. Soc. Dalton Trans. (1972) 102.
[114] J. Skoweranda, W. Wieczorek, M. Bukowska-Strzyżewska, A. Grodzicki, E. Szłyk, J. Cryst. Spectr. Res. 22 (1995) 527.
[115] Z. Zhang, E. Szłyk, G.J. Palenik, S.O. Colgate, Acta Cryst. C44 (1988) 2197.
[116] M. Preisenberger, A. Schier, H. Schmidbaur, J. Chem. Soc., Dalton Trans. (1999) 1645.
[117] P. Römbke, A. Schier, H. Schmidbaur, Z. Naturforsch. 57b (2002) 605.
[118] P.G. Jones, Acta Cryst. C40 (1984) 1320.
[119] P. Schwerdtfeger, P.D.W. Boyd, A.K. Burrell, W.T. Robinson, M.J. Taylor, Inorg. Chem. 29 (1990) 3594.
[120] K.-M. Chi, K.-H. Chen, S.-M. Peng, G.-H. Lee, Organometallic 15 (1996) 2575.
[121] L. Zanotto, F. Benetollo, M. Natali, G. Rosetto, P. Zanella, Chem. Vap. Deposition 10 (2004) 207.
[122] Y. Morishige, S. Kishida, Appl. Phys. A 59 (1994) 395.
[123] M. Karsi, A. Reynes, R. Morancho, J. Phys. IV 3 (1993) 273.
[124] D.A. Edwards, R.M. Harker, M.F. Mahon, K.C. Molloy, J. Mater. Chem. 9 (1999) 1771.
[125] E. Szłyk, P. Piszczek, A. Grodzicki, A. Goliński, J. Szatkowski, T. Błaszczyk, Chem. Vap. Deposition 7 (2001) 111.
[126] P. Piszczek, E. Szłyk, M. Chaberski, C. Taeschner, A. Leonhardt, W. Bała, K. Bartkiewicz, Chem. Vap. Deposition 11 (2005) 53.
[127] T. Hasse, K. Kohse-Höinghaus, B. Atkan, H. Schmidt, H. Lang, Chem. Vap. Deposition 9 (2003) 145.
[128] H. Schmidt, Y. Shen, M. Leschke, Th. Hasse, K. Kohse-Höinghaus, H. Lang, J. Organomet. Chem. 669 (2003) 25.
[129] T. Ogura, Q. Fernando, Inorg. Chem. 12 (1973) 2611.
[130] C.D.M. Beverwijk, G.J.M. van der Kerk, A.J. Leusink, J. Noltes, J. Organomet. Chem. Rev. 5 (1970) 215.
[131] G.D. Roberts, E.V. White, Org. Mass Spectr. 16 (1981) 564.
[132] E. Szłyk, P. Piszczek, M. Chaberski, A. Goliński, Polyhedron 20 (2001) 2853.
[133] W. Lin, T.H. Warren, R.G. Nuzzo, G.S. Girolami, J. Am. Chem. Soc. 115 (1993) 11644.
[134] M.M. Banaszak Holl, P.F. Seidler, S.P. Kowalczyk, F.R. McFeely, Inorg. Chem. 33 (1994) 510.
[135] F. Jansen, T. Kruck, Adv. Mater. 3 (1995) 297.